High Altitude Propeller Design and Analysis Overview

Article · January 2001

Source: CiteSeer

CITATIONS
29

READS
2,170

1 author:

Anthony J Colozza
NASA Glenn Research Center / HX5
118 PUBLICATIONS **1,051** CITATIONS

SEE PROFILE

High Altitude Propeller Design and Analysis Overview

Anthony Colozza
Federal Data Systems
Cleveland Ohio 44135
March 1998

Table of Contents

1. Introduction

The use of a propeller to generate thrust for subsonic flight dates to the beginning of powered flight. The application of propellers to generate thrust under most flight conditions is well understood due to this long history of use and development. However, in certain areas of flight such as high altitude applications, the history of propellers is sparse if not entirely absent. There has been very little work done in the design and construction of propellers that are capable of operating within this regime. This regime is unique because it requires the propeller to operate within a low Reynolds number high subsonic Mach number flow field. Also if the same propeller is used for takeoff and climb then it must be capable of operating over an extremely large change in atmospheric density. These two concerns are the main obstacles to designing and constructing a propeller for high altitude low speed applications.

High altitude subsonic flight is of interest to the atmospheric science community. This type of flight will enable the collection of data in regions of the atmosphere which are not presently well understood. This data can then be used to help determine if any environmental damage has been or is being done. The upper atmosphere is of prime interest to atmospheric scientists due to the large amount of active chemistry that takes place in this region. The most widely known aspect of this is the ozone layer whose recent thinning due to interaction with chlorofluoro-carbons is the cause of great environmental concern. Because of these concerns the Environmental Research and Sensor Technology Program (ERAST) was started by the NASA office of Aeronautics. This program is to develop technologies which will enable safe and cost effective environmental research in the upper atmosphere. There are two main objectives of the Environmental Research Aircraft and Sensor Technology (ERAST) program: to advance the state-of-the-art in UAV capabilities and sensor technologies so that, when used in combination as an integrated science platform, the data collection requirements of the science community are achieved. The second objective is to assist the emerging U.S. UAV industry to be economically viable through cooperation and effective technology transfer[1].

The desired flight altitude and aircraft cruising speed for the proposed ERAST mission would require a propeller to operate in the low Reynolds number high subsonic Mach number regime mentioned above. Therefore, an investigation into the problems associated with the design and performance analysis of a propeller capable of operating within this regime was initiated. The effort was separated into three main categories:

- The examination of any propellers which were previously designed for operation within a similar flight regime and the level of effort and scope required to design this type of propeller.

- An investigation into the ability to provide performance estimates of a given propeller design under these high altitude flight conditions by using computer code analysis.

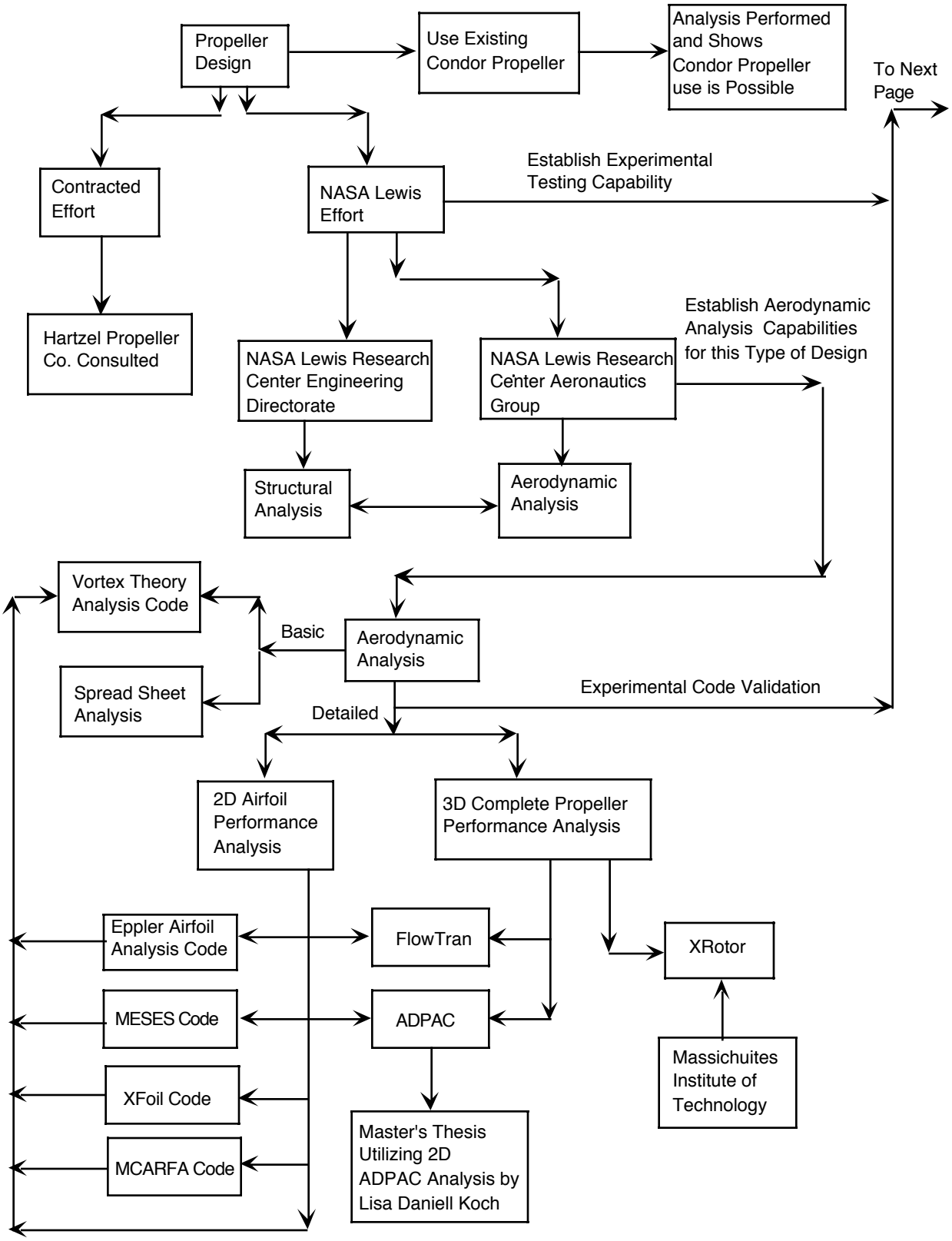

Figure 1a. High Altitude Propeller Task Flow Chart

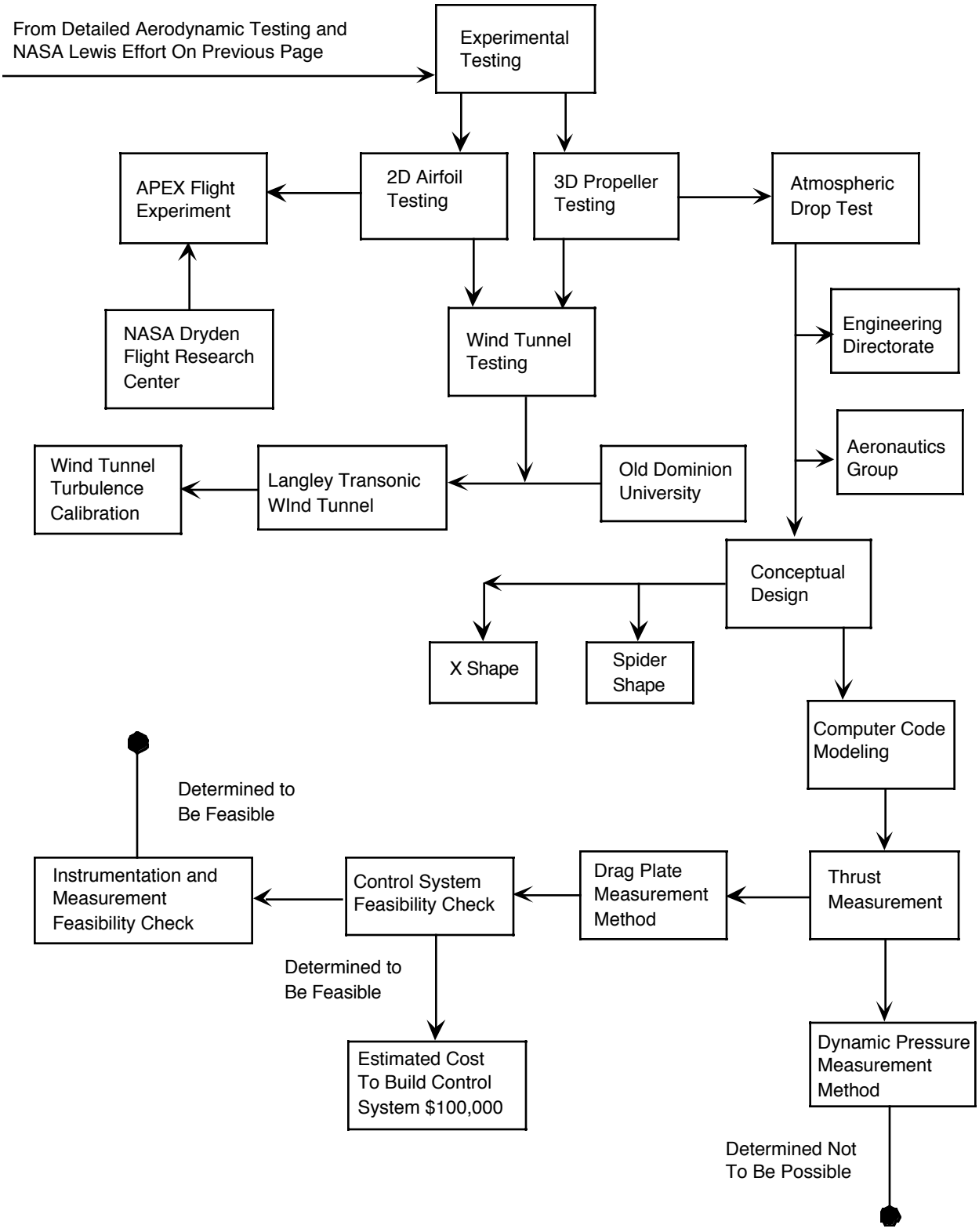

Figure 1b. Continuation of High Altitude Propeller Task Flow Chart

• An investigation into providing performance data through experimental testing.

Based on these three categories a number of tasks were performed. These tasks and the findings that resulted are included within this report. A flow chart of the tasks which were performed and the organizations involved was made to show graphically how the various items are interconnected and the method for investigating each of the three main categories (design, analysis and experimentation). This flow chart is shown in figures 1a and 1b.

2. Background

There is not a lot of history related to the design of high altitude propellers. The maximum flight altitudes which have been achieved using propeller driven aircraft are 20.4 km (67,000 ft) on a combustion driven aircraft (Condor) and 21.3 km (70,000 ft) for solar electric aircraft (Pathfinder). Although there is no direct historical reference to the use of propellers at altitudes between 24.4 km (80,000 ft) and 30.5 km (100,000 ft), the examination of those designed for lower altitudes could still provide valuable information on performance and design issues that should be applicable to higher altitude propellers. A brief description of some propeller driven high altitude aircraft which have flown is given below.

Condor

The Condor aircraft which was a high altitude unmanned military demonstration aircraft constructed in the late 1980's for reconnaissance. It presently holds the record for high altitude internal combustion driven propeller flight at 20.4 km (67,000 ft). The propeller used in the condor was designed by Hartzell Propeller Co. of Piqua OH. It's a variable pitch three bladed propeller.

TEXT OMITTED DUE TO EXPORT CONTROL

FIGURE 2 OMITTED DUE TO EXPORT CONTROL

The structural testing on these blades was very comprehensive. Numerous tests were performed to insure the integrity of the blade and to verify the construction techniques used. Free body shaking tests were performed in order to determine the blades resonant frequencies. Resonant frequencies were found at 9, 28, 38, 62 and 80 Hz. TEXT OMITTED DUE TO EXPORT CONTROL

Perseus Series

The Perseus B, shown in figure 3, was designed as an unmanned reconnaissance vehicle capable of flight up to 24.4 km (80,000 ft). To date it has reached an altitude of 15.2 km (50,000 ft). The flight to 15.2 km (50,000 ft) used a 2.8 m (9.2 ft) diameter propeller. This is not the same propeller which was designed for use at 24.4 km (80,000 ft). To date the high altitude propeller has been used to altitudes up to 12.2 km (40,000 ft). The high altitude propeller has 2 blades and is 4.4 m (14.4 ft) in diameter. It is constructed of a tubular spar with a light weight composite shell and is designed to absorb 50 kw (67 hp) of power at altitude. The propeller pitch is actuated by an electric motor. When this motor is inactive a break locks the blades at their current pitch. This breaking system enables the electric motor to be shut down when not in use. The propeller blades weigh approximately 7 kg (15.5 lb) and the pitch control mechanism weighs approximately 3 kg (6.5 lb). The perseus propeller was designed using the Xrotor propeller code developed at MIT.

Figure 3 Perseus B Aircraft at Dryden Flight Research Center (NASA photo EC96 4344083)

The Perseus B is powered by a 3 stage turbocharged Rotax 912 engine designed to produce 80 hp at altitude. This design originated with the Perseus A, which was a similar aircraft except with a closed cycle internal combustion engine.

Caproni 161

The propeller driven Caproni 161 aircraft reached 17 km (56,000 ft) in 1938. This aircraft was an experimental biplane. It carried 1 pilot and was powered by 1 512 kW engine. Little information however could be found on the propeller used in this aircraft.

Strato 2C

The Strato 2C, shown in figure 4, is a high altitude manned aircraft used for environmental research. It uses two 5 bladed variable pitch propellers with a diameter of 6 m (19.7 ft). The propellers are constructed with a wooden spar and a composite shell. The propeller pitch is controlled by a hydraulic governor which is driven by the propeller gearbox and integrated into the gearbox oil system. Due to the fairly low cruise RPM (approximately 640) a conventional feathering system with counter weights was not used. Instead an all hydraulic system is used. This system has a separate emergency feathering pump supplied with oil out of a separate volume in the gearbox oil sump. The propeller is designed to absorb 300 kW (400 hp) of shaft power from the engine.

Figure 4 Strato 2C Aircraft

Pathfinder

The Pathfinder aircraft, shown in figure 5, constructed by Aerovironment Inc. holds the present altitude record for propeller driven aircraft at 21.8 km (71,530 ft). This aircraft is solar powered and uses 6 dc electric motors for propulsion The propellers are fixed pitch and 2 m (6.56 ft) in diameter. They are constructed utilizing a spar / rib method with an outer shell covering. The construction materials are Kevlar 285C cloth for the outer covering and unidirectional fiber glass for the spar caps. There is a 50.8° twist in the blade from the root to the tip.

Figure 5. Pathfinder Aircraft

Grob EGRETT

The Grob EGRETT is an atmospheric science aircraft built by the Grob company of Germany. It is shown in figure 6 [2]. It is 2 person, single engine propeller driven aircraft powered by a Garrett turboprop engine. The maximum altitude it has reached was 16.5 km (54,000 ft) in 1988. The payload capacity of the aircraft is 750 kg. It can maintain an altitude of 15km (50,000ft) for approximately 8 hours. The cruising speed at altitude is Mach 0.45 giving it a range of approximately 2800km (1500NM) .

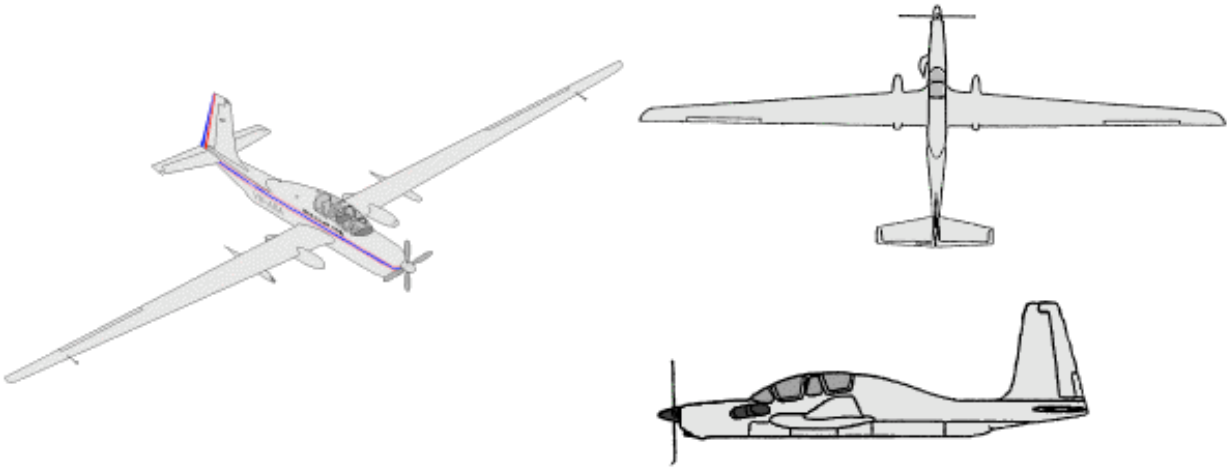

Figure 6 Grob EGRETT Aircraft Diagram [2]

The Egrett series of aircraft was originally developed by Grob Flugzeugbau GmbH & Co KG (Germany) and E-Systems Inc. (USA) as a low cost, high altitude reconnaissance platform for the German and US Air Forces. A total of five airplanes were built, the single-seater Proof-of-Concept aircraft, three

production single seaters and one two-seater trainer. After an evaluation period, the two Air Forces decided that the aircraft did not fit their requirements. Since then,
some of the single seaters have been successfully used as ad-hoc high-altitude research platforms (by Aurora Corporation in the USA and by the Weltrauminstitut in Berlin). [2]

3. Design Approach

The main object in the design of a propeller is to transfer the power produced by the engine to the air stream as efficiently as possible. For a propeller to operate at high altitudes there are a number of unique design issues that must be addressed. The ability to transfer power to the air stream is directly proportional to the density of the air the propeller is operating in. For a given rpm the horsepower absorbed by the propeller and transferred to the air stream at 24.4 km (80,000 ft) will be about 1/30th that absorbed at sea level. Aside from the geometry (airfoil and blade twist) of the propeller blade there are two main factors which will significantly affect the performance of the propeller at a given altitude. These are the propeller's diameter and RPM. RPM is limited by propeller tip Mach number constraints. For a typical propeller design the tip Mach number limit is around 0.75 Mach. This is done to avoid the formation of shock waves on the propeller blade. Shock waves can have a number of adverse effects on the performance of the propeller. Due to the pressure gradient through the shock wave the drag of the propeller blade can increase significantly. Also since most propeller blades are fairly flexible once a shock wave forms the change in the pressure field on the surface of the blade can cause the blade to twist thereby allowing the shock to travel along the blade section. This motion of the shock wave over the surface of the blade can initiate a fludder in the blade which can severely reduce its performance if not destroy the propeller. This relationship between the allowable RPM and diameter is shown in figure 7. Because of the restrictions on RPM the most effective way of increasing the output power of a propeller is by increasing its diameter.

Another issue in designing a propeller for high altitudes is that the aircraft will most likely need to be capable of taking off from the ground and climbing under its own power to the desired altitude. This means that the propeller must be capable of operating over an extremely large range of atmospheric densities. Also since the diameter of most high altitude propellers is fairly large in order to generate sufficient thrust at altitude their ability to be used during takeoff may not be possible. Sufficient ground clearance may not be achievable with a conventional aircraft design and takeoff approach. Due to these issues some less conventional propeller concepts have been examined to see if they would be appropriate for a high altitude aircraft.

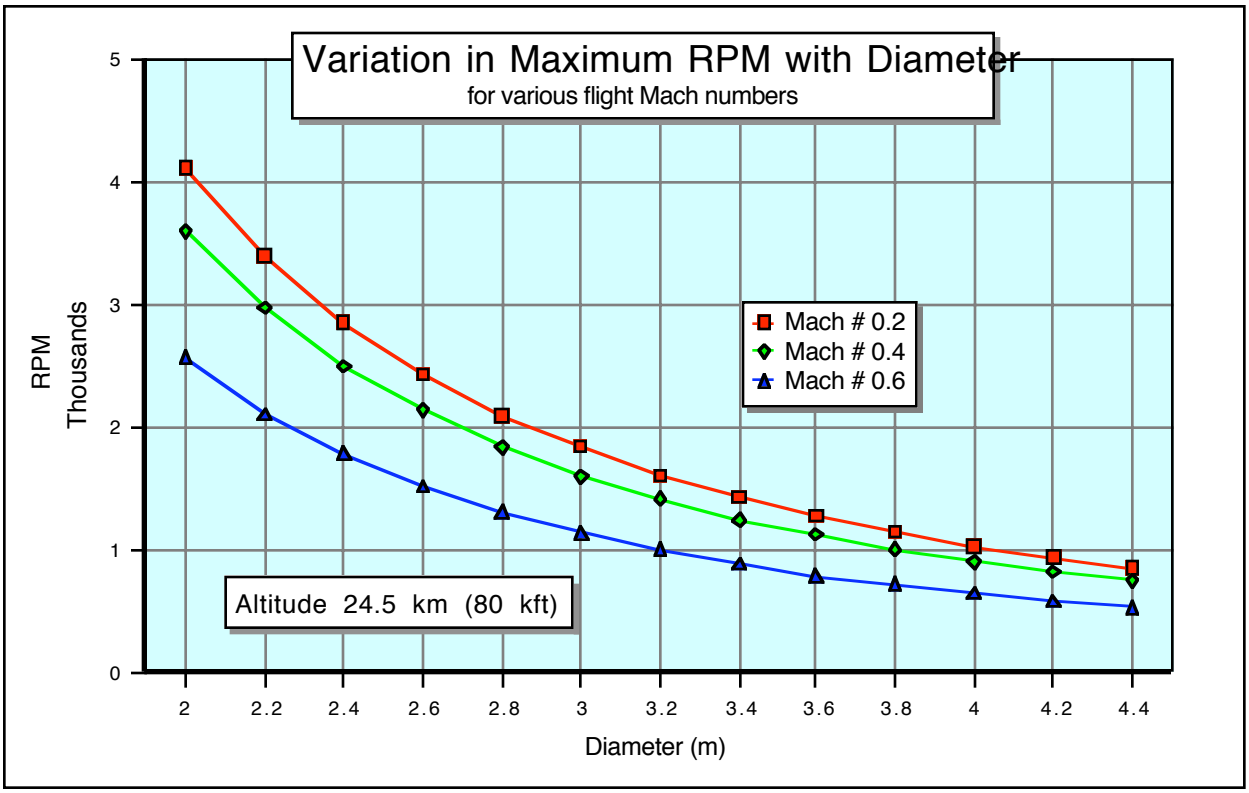

Figure 7 The Effect of Propeller Diameter on RPM

Variable Diameter Propeller

Sikorsky Aircraft has recently done work on developing a variable diameter propeller for a tiltrotor aircraft[3,4]. The ability to vary the diameter of the propeller throughout the flight would have significant benefits for a high altitude aircraft. As the air density decreases the diameter could increase in order to keep the thrust generated constant. It would also aid in take off and landing by reducing the ground clearance needed by the aircraft. However, the present state of the art of this type of propeller does not lend itself toward use on a light weight high altitude aircraft. The propeller presently under development is for a vertical takeoff and landing aircraft. The requirements for this aircraft are much different then those of a high altitude aircraft therefore the weight and power absorption capability of this propeller would not be applicable. Also the present propeller is capable of extending its diameter approximately 30%, for high altitude aircraft applications the presentage increase would need to be greater on the order of 50% or more. It is possible to continue development of the concept toward a propeller which would be usable by a high altitude aircraft however the cost and timeframe associated makes this development prohibitive for use with the ERAST program. Although this concept is interesting, due to its present state of early development and lack of synergy with present development programs this concept cannot be considered as a viable alternative to a conventional propeller system.

Dual Propeller Concept

The dual propeller concept is based on the premise that if you use two separate propellers, one designed for low altitude operation and one designed for high altitude operation, then the overall propulsion efficiency will increase throughout the complete altitude range of the aircraft. By reducing the altitude range the propeller has to operate within, the propeller design can be tailored to give higher efficiency. A side benefit to this concept is that it allows for easier takeoff since only the smaller low altitude propeller needs to be used thereby reducing the necessary ground clearance. This concept is particularly applicable to an aircraft that has only one or two engines / propellers. The greater the number of engine / propellers that are used the smaller the required propeller diameter. So as the number of engine / propellers increases the advantage of using a dual propeller system decreases.
Figure 8 shows how the number of engines / propellers effect the required propeller diameter necessary to produce a given thrust level.

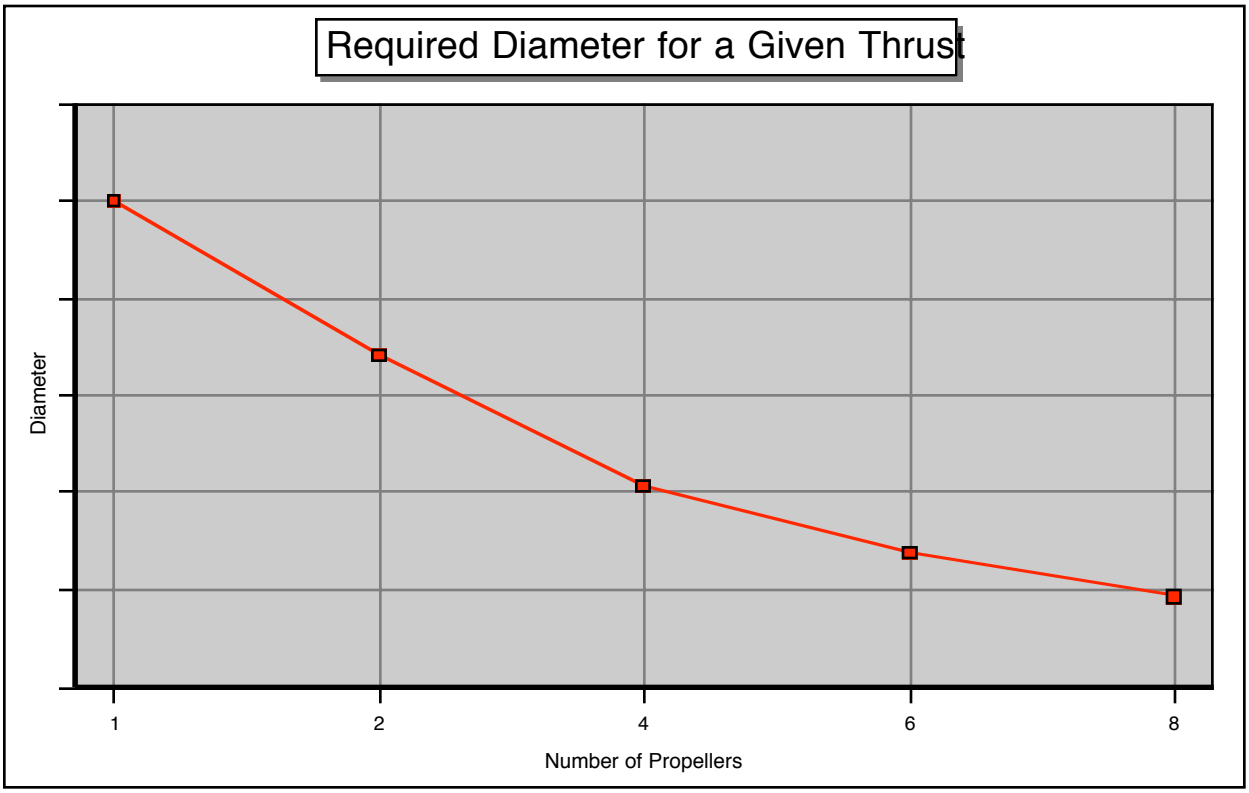

Figure 8 Propeller Diameter Versus Number of Propellers

A dual propeller system would operate by having the large propeller fixed in a horizontal position during takeoff and landing. The smaller propeller would be used for take off and climb to some predetermined design altitude. After takeoff the large propeller would be released and left to freely rotate with the blades in the feathered configuration in order to minimize drag. Once the initial design altitude for the larger propeller was reached it would be locked to the drive shaft

and the pitch angle adjusted to its proper setting. The smaller propeller would be left to rotate with the larger propeller although its contribution to the thrust generate would decrease significantly as the aircraft continued to climb in altitude.

One of the main drawbacks to the dual propeller concept is the extra weight and complexity of the dual propeller system. A dual shaft is needed which would allow the large propeller to rotate independently of the smaller propeller. The large propeller must also be capable of rotating freely of the drive shaft and therefore must have a clutch mechanism to engage and disengage it from the drive shaft. Both the large and small propeller would each need their own pitch control mechanism. And finally the control system needed to operate the dual propeller system would be much more complicated then that used for a single propeller system.

The issues mentioned above need to be addressed during the design of both the propeller and aircraft. These issues will influence various aspects of the aircraft's design and operation which include: the proposed takeoff and landing scheme for the aircraft, the ground clearance of the aircraft, the location of the propulsion system(s) and the number of engines / propellers on the aircraft. Based on these issues there are a number of design tradeoff related to the propeller performance which need to be considered during the aircraft design phase. Some of these tradeoffs are illustrated in figures 9 through 13.

The effect of multiple engine/propeller systems on the propeller diameter can be seen in figure 8. This figure assumes that the same amount of thrust is needed regardless of the number of engine/propeller systems which are used. In other words adding up the thrust generated by each propeller in a 4 engine aircraft will be the same as that generated by the single propeller in a single engine aircraft. There are some positive and negative effects of reducing the propeller diameter by utilizing multiple engines. The maximum RPM the propeller will be capable of operating at will increase as the diameter is decreased, as shown in figure 7. This has a positive effect on the propeller performance since the propeller can now run at a higher Reynolds number. However the efficiency of the propeller and its output thrust will decrease as the diameter is decreased. This is shown in figures 9 and 10.

The aircraft mission characteristics will also affect the performance of the propeller. As the required mission altitude is increased the propeller output power will decrease. This effect is shown in figure 11. The required aircraft cruise velocity also affects the propeller performance. Figure 12 shows the propeller efficiency as a function of aircraft cruise velocity. From this figure it can be seen that there is a velocity range which will produce the highest efficiency for the propeller. Above and below this range the propeller efficiency drops off. The effect of cruise velocity on output thrust of a given propeller can be seen in figure 13. There is an optimum cruise velocity which will produce the maximum thrust for a given propeller.

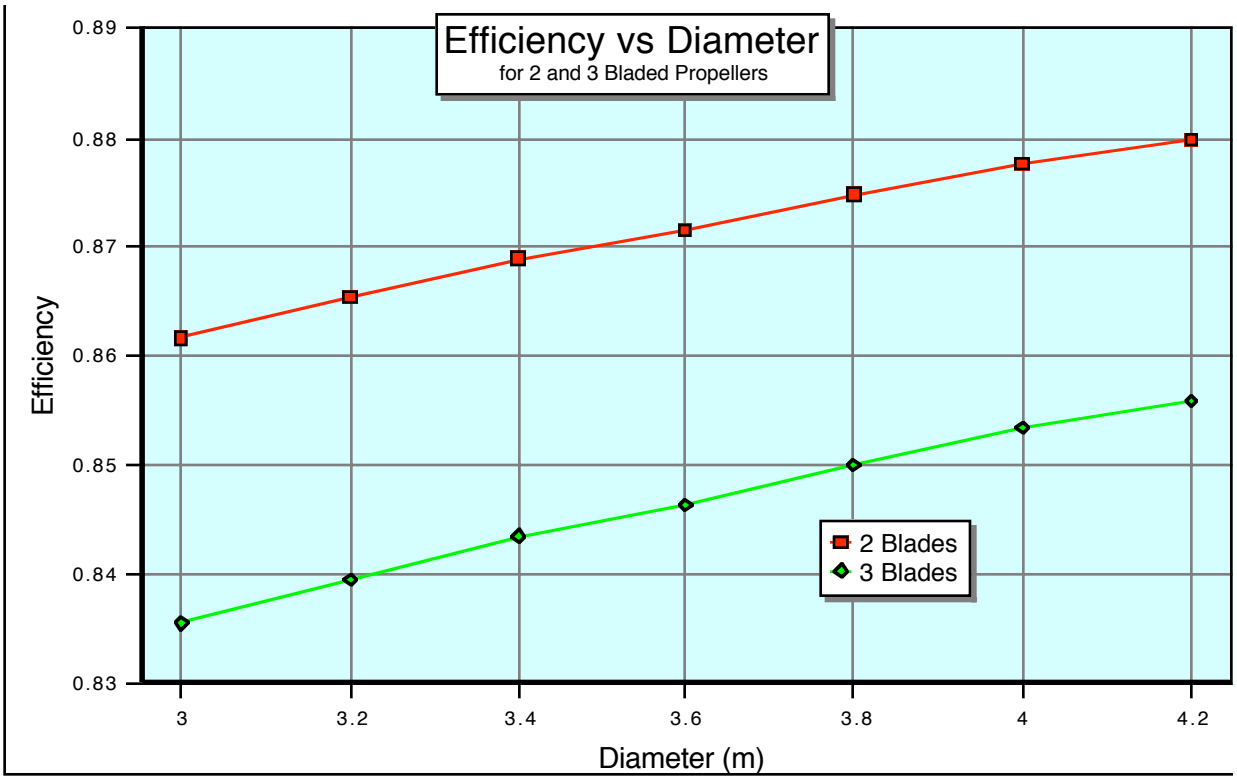

Figure 9 Effect of Propeller Diameter on Propeller Efficiency

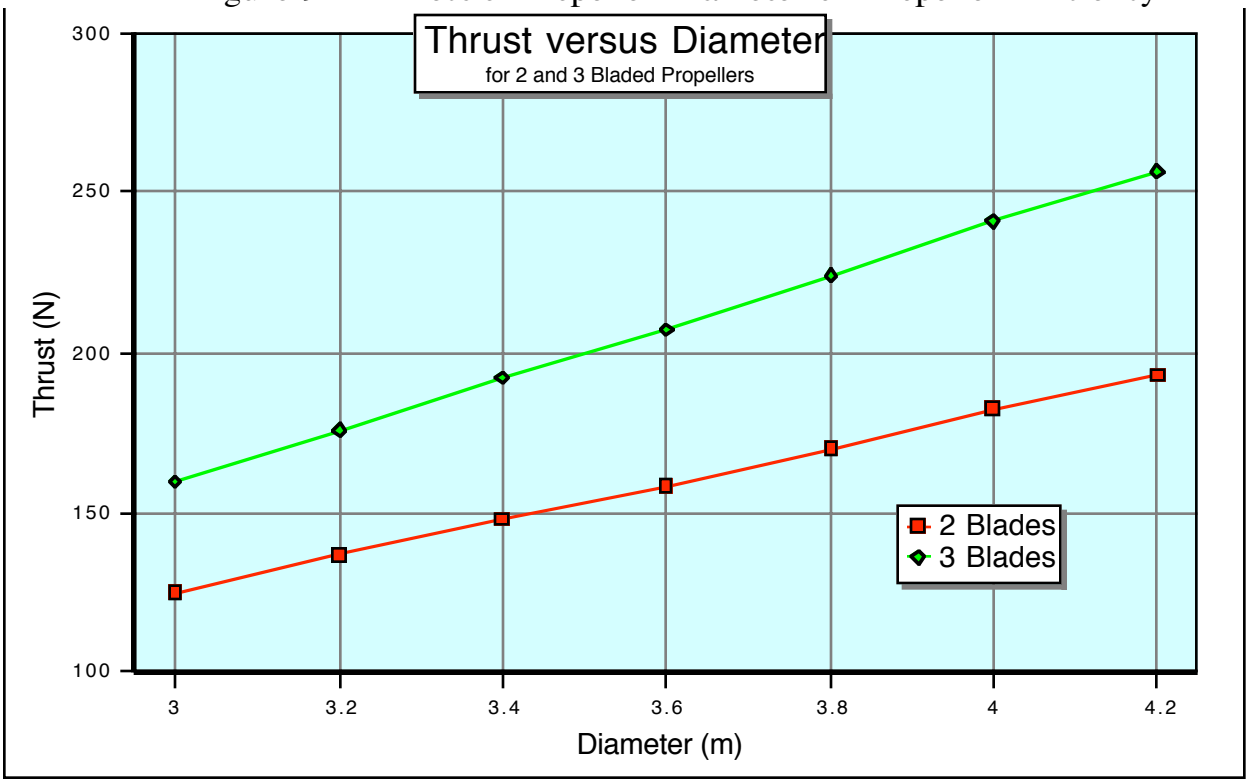

Figure 10 Effect of Propeller Diameter on Output Thrust

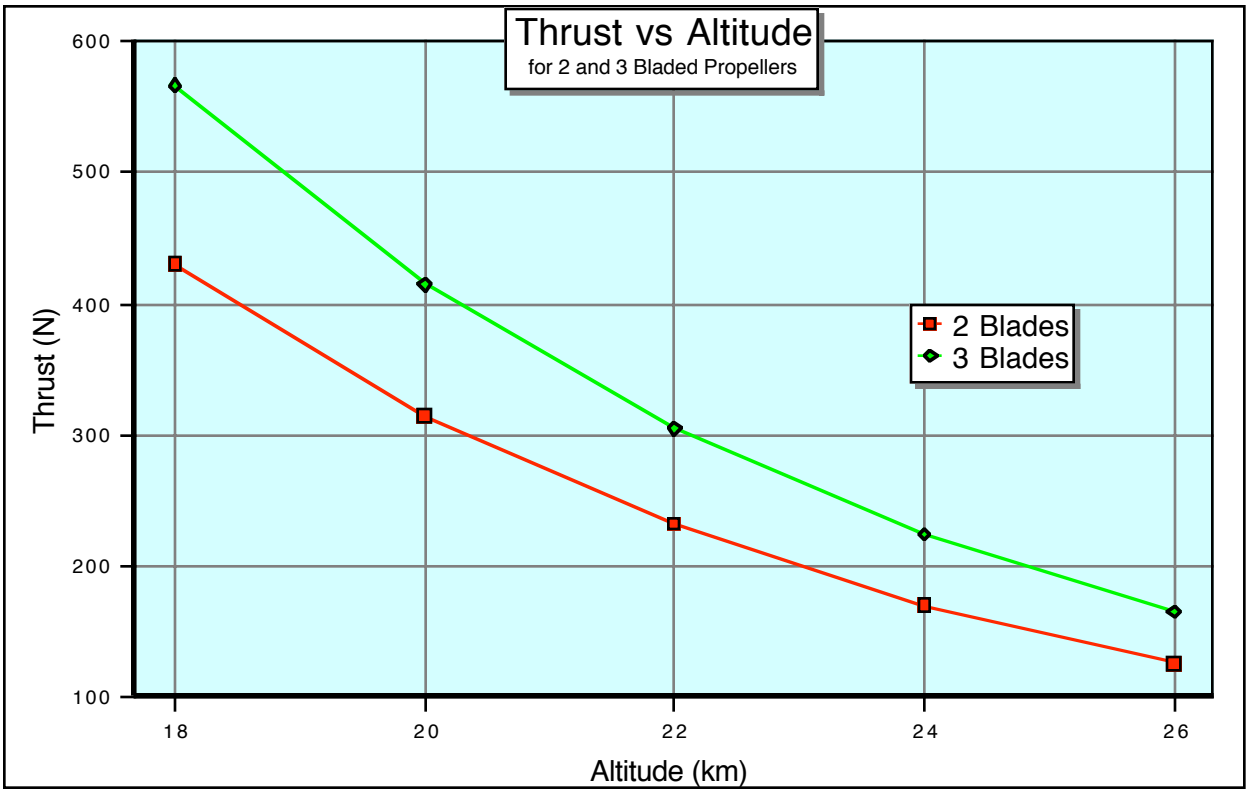

Figure 11 Effect of Altitude on Output Thrust

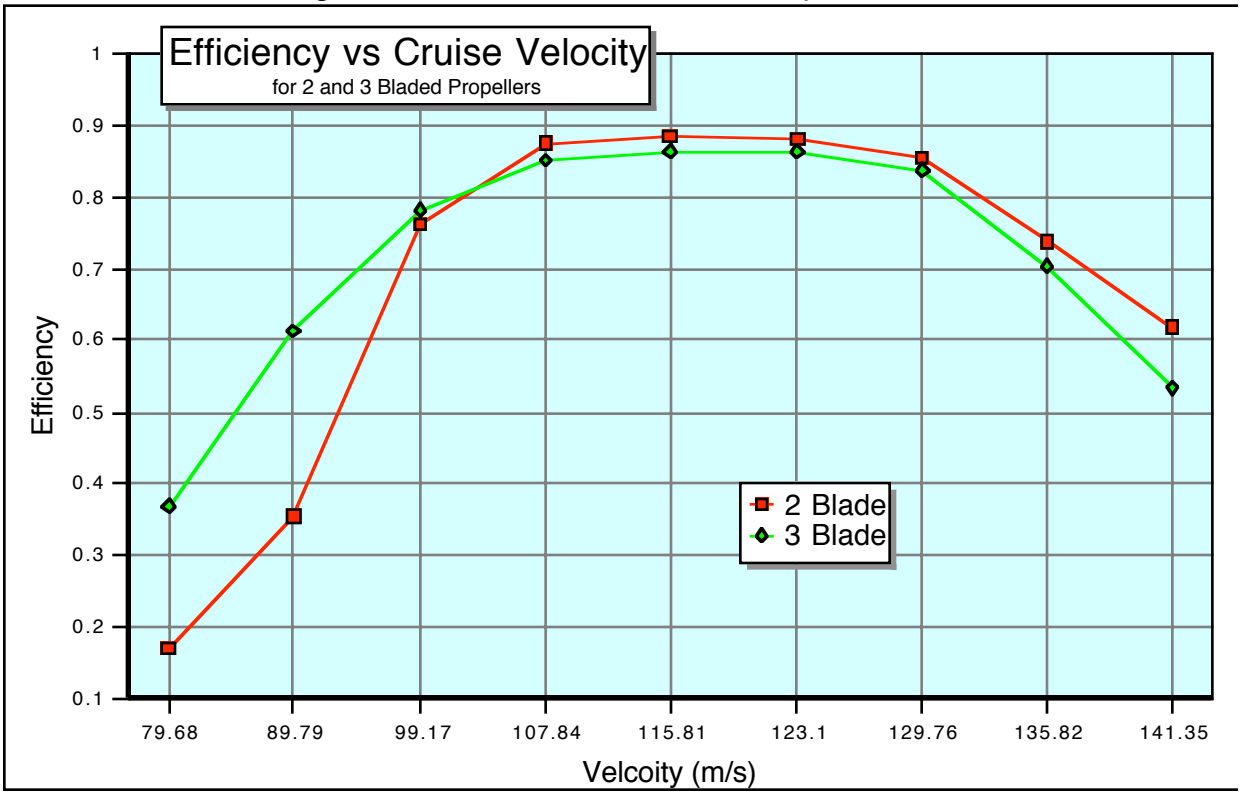

Figure 12 Effect of Cruise Velocity on Propeller Efficiency

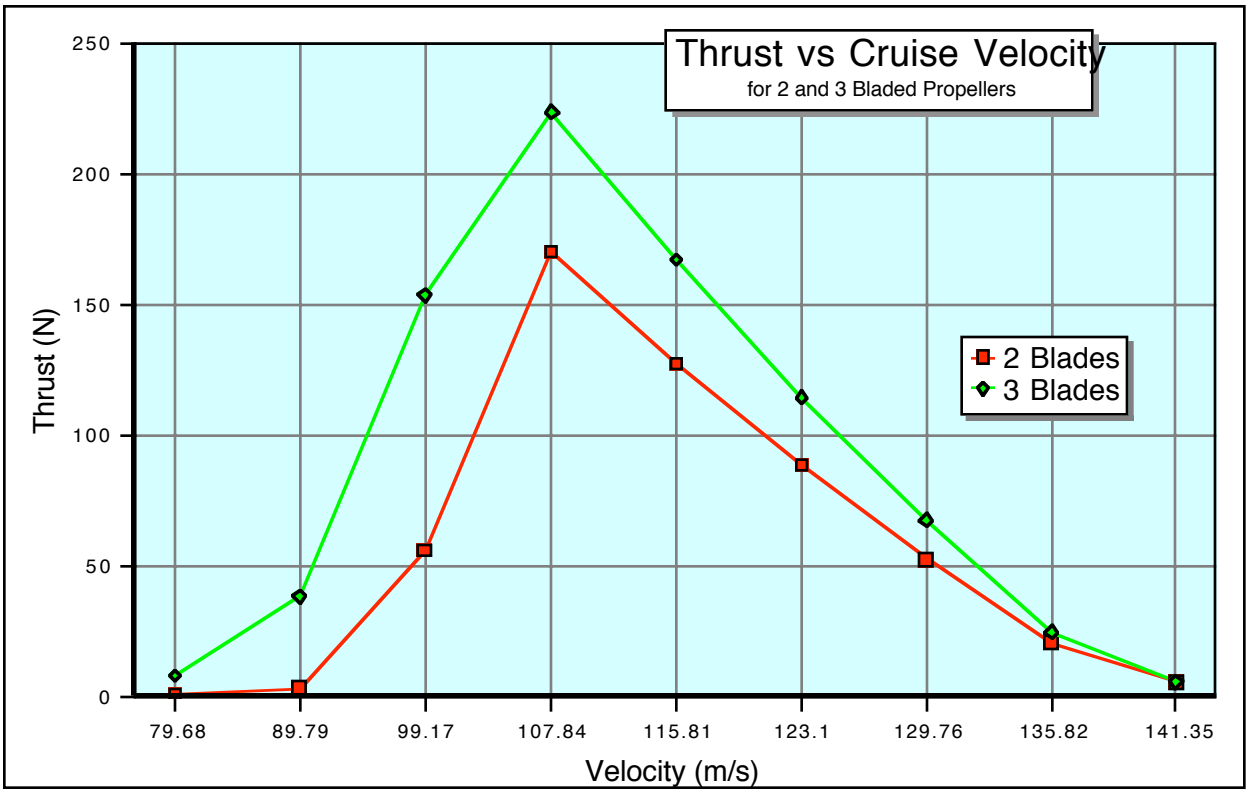

Figure 13 Effect of Cruise Velocity on Propeller Thrust

3.1 NASA Lewis Proposed Design Approach

The development of a propeller capable of operating at altitudes up to and exceeding 24 km (80,000 ft) is part of the objectives necessary to meet the mission goals of the ERAST program. A plan to accomplish this propeller development was established. The initial plan consisted of determining what was needed and the resources required to achieve the following main elements:

- Establish the analysis and design capabilities necessary for the development of a high altitude propeller.
- Construct and test a prototype propeller.
- Determine the operational torque profiles for a high altitude propeller which are to be used in conjunction with a ground test simulation of the complete propulsion system.

Based on the outcome of the requirements necessary to achieve the goals listed above a decision would be made as to whether to proceed or not. The first goal of establishing the ability to determine propeller performance for both an existing or proposed propeller blade consisted of determining what computer

codes could be used and what experimental methods are available.

For the computer code analysis both a structural and aerodynamic analysis capability is necessary. This is due to the flexing of the blade during operation. Sufficient analysis capabilities exist to perform a structural model of the propeller under any aerodynamic loading configuration. If the material makeup of the propeller and the aerodynamic loads applied are known. In order to determine these loadings a detailed aerodynamic model must be done. The aerodynamic analysis capabilities are discussed in detail in sections 4. To perform an accurate estimate of the propellers performance these structural and aerodynamic models must be performed in conjunction with each other in an iterative process. This analysis capability can be used to either determine the performance of an existing propeller or to assist in the design of a new propeller.

If the computer analysis capabilities cannot be established to a degree which would assure the development of a propeller with the desired performance then an experimental analysis would need to be done. A detailed description of the experimental analysis approach is given in section 5.

Once the analysis capability is established then the design and construction of a propeller can be done. It was estimated that to set up the analysis capabilities, design and construct a propeller in house at the NASA Lewis Research Center the cost would be on the order of $1 million dollars. It should be noted that this cost estimate does not include any aerodynamic, mechanical hub or spin testing hardware design, analysis or fabrication. Also this estimate assumes the use of aerodynamic computer analysis that has not yet been established. The timeline estimated for producing this prototype propeller is approximately 2 years barring any major obstacles.

The final objective to provide characteristic torque curves for a high altitude propeller can be accomplished once the analysis capability mentioned above is established and a propeller design is available. If no specific design is available then a general performance estimate can be made based on an existing propeller such as the CONDOR's. Details on the CONDOR propeller are given in section 3.3.

3.2 Hartzell Design

Hartzell Propeller Co. was established in 1917 and is located in Piqua, Ohio. They have a significant history designing propellers for all types of aircraft. Some of the more unique propeller designs they have produced include the propeller for the Voyager aircraft, which set the aircraft endurance record by flying nonstop around the world, the CONDOR aircraft described in section 2, and the Pond Racer, an aircraft designed to break the world speed record for piston powered flight.

Due to their work with the CONDOR aircraft Hartzell was contacted to see

if they had interest in designing and constructing a propeller for the ERAST aircraft. Based on their past experience and the company's interest in producing high profile unique propeller designs they indicated they were interested. However, most of the personnel involved with the CONDOR propeller design had either left the company or moved into other positions within the company not directly involved with propeller design.

The CONDOR propeller was a unique one of a kind design. It was unlike any of Hartzell's previous production propellers. The propeller designed for the ERAST aircraft would have to be done with a similar approach. Because of this they estimated the cost would be around $1 million dollars. They indicated that they do not make much profit from this type of limited production propeller. They also estimated the time frame for producing the propeller would be on the order of 12 to 18 months. This cost did not include any testing of the propeller other then some static structural testing. As was the case with the CONDOR propeller, they do not have the facilities to test this type of propeller under any operational conditions.

3.3 The Condor Propeller

Due to the mission similarities between the Condor and the proposed ERAST aircraft the possibility of directly using the Condor propeller for the ERAST high altitude aircraft has been considered. This section addresses the feasibility of this concept using the Condor performance data which was available.

The Condor aircraft and all the associated data from its design and testing was stored at Lawrence Livermore Laboratory for a period of time. The aircraft has since be moved from this storage facility and all of the hardware and documentation are no longer at a single location. However, during this storage period at Livermore a number of people from NASA Lewis Research Center went there to try and recover as much data as possible from the Condor program. Among the documents recovered were those related to the design and operation of the propeller. Included in the data was a map of the propeller performance generated by Hartzell. Based on this map it seems possible that the Condor propeller could be used for the ERAST mission profile. It should be noted that the map from Hartzell was produced from analytical calculations not experimental data. Hartzell never tested the propeller due to its size and proposed flight regime.

The Condor aircraft was a high altitude unmanned military demonstration aircraft constructed in the 1980's. Its mission was to perform high altitude reconnaissance and the maximum altitude it achieved was 20.4 km (67,000 ft). The propeller used in the Condor is a variable pitch three bladed propeller TEXT OMITTED DUE TO EXPORT CONTROL

The propeller map, shown in figure 14, is for the three bladed Condor propeller. The solid lines are the actual Hartzell map; the dashed lines represent

a "crude but most likely" extrapolation of the map's known contours. Due to the higher maximum flight altitude of the ERAST aircraft and corresponding increased airspeed the operational advance ratio and power coefficient for the propeller will likely fall into this extrapolated region of the map for the higher altitude operation. For the ERAST application it is possible to use the propeller in either a 3 or 2 bladed configuration. There will be a slight efficiency change in going from a 3 bladed to a 2 bladed propeller. However this will be small and for initial estimations can be ignored. The main difference between the 2 and 3 bladed propeller is that for the same flight conditions and engine output power the 2 bladed propeller will have to operate at a pitch angle approximately 2° higher then the 3 bladed propeller to generate the same amount of thrust.

Presently the only data we have on the Condor propeller is the thruster map that was supplied to Boeing by Hartzell and the flight performance data that was reported in Boeing's MDS final report[5]. This document includes a propeller wake survey pressure data but not direct measurements of propeller thrust. The relevant pages from the MDS final report are given in appendix A. Generally speaking, Boeing's comments on the propeller map data supplied by Hartzell indicate that at high altitude and high power levels the map reflects the observed performance while at low altitudes the map seemed to be optimistic.

Additional data on the structure and design of the Condor propeller was requested from Hartzell but to date they have been reluctant to give out any of this information. The geometry of an actual Condor blade, which was acquired from storage at Livermore, was mapped (blade airfoil contours, twist, etc.). This geometry data is given in appendix B. With this blade contour information it may be possible predict the propeller's performance at our extreme flight conditions with a computer model rather then extrapolating performance from the vendor's map which is the only course at present. The airfoil modeling codes which could possibly be used for this task are given in section 4.

Based on the size of the propeller and the flight altitude some information can be generated on the performance limits of the propeller. By restricting the tip Mach number of the propeller and selecting an aircraft velocity, data on the maximum allowable RPM and corresponding advance ratio can be determined. This data is plotted in figure 15. The estimated propeller output horsepower can also be generated as a function of power coefficient, c_p, and advance ratio. This data was plotted over the propeller map found in the Hartzell data. These plots, shown in figures 16 and 17, were generated for altitudes of 24.4 km (80 kft) and 24.9 km (85 kft). With these three sets of curves the performance of the Condor propeller can be estimated and its applicability to the ERAST mission can be assessed. For the ERAST flight altitude goal of 24.4 km (80 kft) the Condor map indicates that the propeller can absorb up to 75 kW (100 hp) with efficiencies greater then 75%. This can be seen from the power absorbed curves in figure 16. This power level is well within the range of operation for the ERAST aircraft. However as the flight altitude increases the amount of power absorbed by the propeller decreases. This is seen in figure 17 for a flight altitude of 24.9 km (85 kft). At this altitude the maximum power absorption of the propeller is

FIGURE 14 OMITTED DUE TO EXPORT CONTROL

around 80 hp with an efficiency less the 75%. In other words the applicability of the Condor propeller to the ERAST aircraft decreases as the desired flight altitude is increased above 24.4 km (80 kft) .

Figures 15, 16 and 17 can be used to estimate the flight performance of the propeller. By selecting the aircraft flight velocity from figure 15, the advance ratio for the propeller is established as well as the maximum allowable RPM. Using this advance ratio, the flight power coefficient, c_p, and propeller efficiency can be found from figures 16 or 17 depending on the desired operational altitude. This is done by moving up the advance ratio line until the desired horsepower line is crossed. (It should be noted these curves are for a 3 bladed propeller. For a 2 bladed propeller the performance values should be similar however the blade pitch angle will be approximately 2° greater). For example, if the aircraft was flying at 110 m/s the advance ratio, **J**, would be approximately 1.8. If the desired horsepower level is 80 hp and the altitude is 80 kft, then from figure 16 the power coefficient would be approximately 0.257 and the propeller efficiency, η , would be approximately 88%. With these values, the thrust generated by the propeller can be estimated.

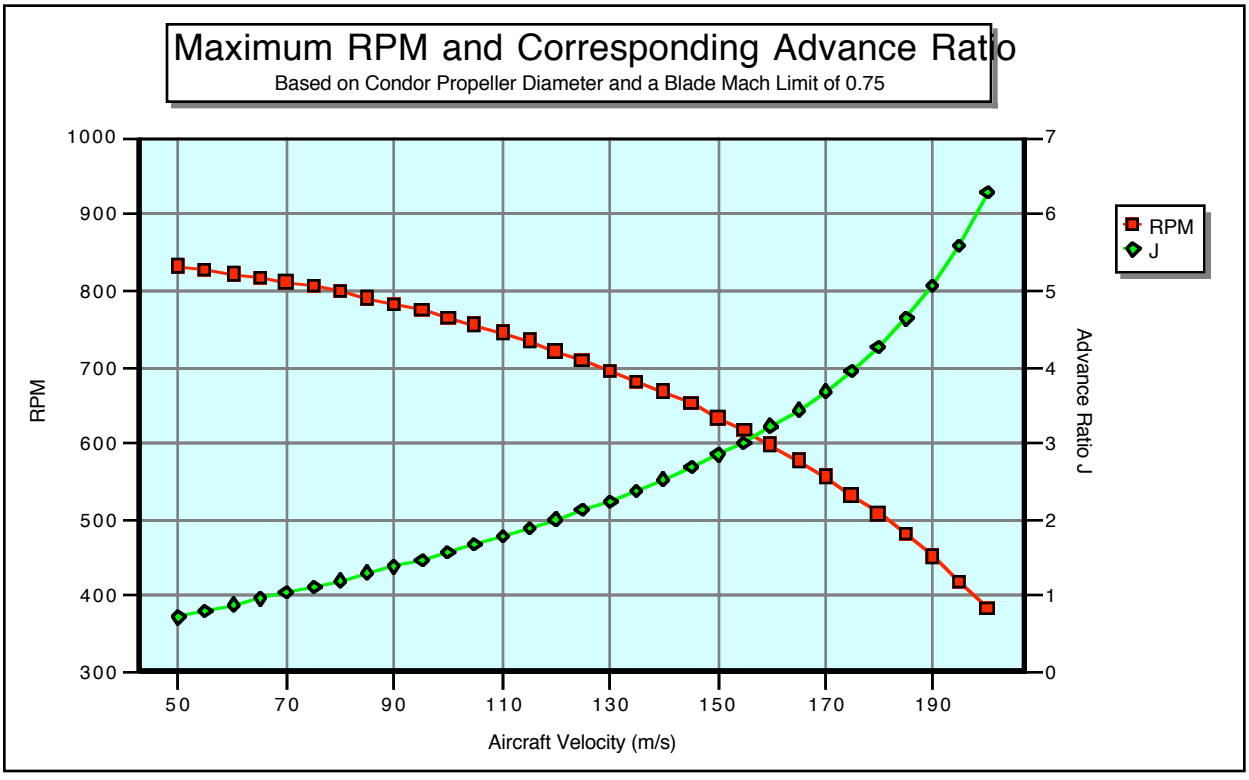

Figure 15 Maximum RPM and Corresponding Advance Ratio for 5 m Diameter Propeller

FIGURE 16 HAS BEEN OMITTED DUE TO EXPORT CONTROL

FIGURE 17 HAS BEEN OMITTED DUE TO EXPORT CONTROL

The thrust coefficient is given by the following relationship.

$$c_t = \eta\, c_p / J \qquad [1]$$

Therefore the thrust coefficient, c_t, is 0.126 (for a c_p of 0.257, η of 0.88 and **J** of 1.8). From this coefficient the thrust generated can be calculated as follows.

$$T = c_t\, \rho\, n^2\, d^4 \qquad [2]$$

Where the propeller diameter (d) is approximately 5 m (16.4 ft). For 80 k ft the atmospheric density (ρ) is 0.0437 kg / m^3 and, from figure 15, the propeller RPM is approximately 750 rpm or 12.5 rps.

$$T = 0.088 * 0.0437 * 12.5^{\,2} * 5^{\,4} \quad = 538\ \text{N} \qquad [3]$$

After substituting in the values the estimated thrust output for the 3 bladed Condor propeller under these flight conditions is 538 N (120 lbf). It should be noted that a 2 bladed version of this propeller can produce the same amount of thrust under the same conditions if it was operated at a pitch angle approximately 2° greater then the pitch angle for the three bladed propeller.

4. Analysis Approach

Performance analysis of a propeller is a wide topic. It can range from a simple spreadsheet analysis to a full 3D flow field analysis of the propeller and the surrounding aircraft. Due to the wide variation in the analysis capabilities the type of analysis selected depends on what questions are trying to be answered. In general the type of analysis can be broken into two categories, basic and detailed.

The basic analysis such as the spread sheet model given in section 4.1.2. is useful for getting a quick estimate of a propellers performance under certain conditions. Little propeller geometry is needed and a rough estimate of performance is obtained. This is valuable for evaluating a number of potential or existing designs for a particular mission in order to estimated their performance and applicability to the proposed mission. Also limits on certain characteristics, such as diameter or activity factor, can be quickly investigated for a given application. This type of analysis is useful in the beginning stages of a design in order to get pointed in the right direction regarding the propeller geometry. A step beyond the spreadsheet analysis is the vortex or strip theory analysis. This type of analysis takes into account the specific geometry of the propeller and is useful for investigating design and off design performance. This type of analysis can be used during the design process in which a number of different geometries are being investigated. Various propeller geometries can be investigated fairly quickly and with reasonable accuracy. It is more time consuming then the

spreadsheet analysis since the computer code would need to be edited whenever the propeller geometry is altered.

Beyond the basic analysis is the detailed analysis. In general this consists of computer codes which model the flowfield around the propeller. With this type of analysis a detailed model of the propellers operation can be generated. There are two categories of these fluid flow analysis codes, 2D codes and 3D codes. The 2D codes cannot be used to model the propeller directly. They can however be used to model the performance of the airfoils used in the propeller. This information can then be used in conjunction with the simpler strip or vortex theory analysis code to obtain increasingly accurate results. There are some significant benefits to this type of analysis approach. Even though the generation of the airfoil data may be time consuming once it is obtained incorporating it into the vortex theory analysis significantly increases the accuracy of the results. This benefit is gained while still maintaining the ease and flexibility inherent with vortex analysis. Beyond this 2D / Vortex theory analysis approach is the full 3D analysis. This type of analysis is the most accurate available. It can be used to model the complete flowfield over the propeller and any surrounding aircraft structure. If is very useful for evaluating a propeller performance at a particular operational point and investigating any performance problems associated with the propeller or installation design. This type of analysis is very intricate and time consuming and requires significant experience in order to produce results which are valuable.

4.1 Basic Analysis

The basic propeller analysis is to utilize computer modeling to quickly analyze a propeller and estimate its performance. This analysis can be done for either a single point of operation or to generate a complete operational map. There are two examples of the basic analysis approach listed in the following sections. The main goal of this type of analysis is to get a performance estimate of a given propeller. There are a number of different approaches to achieving this goal. The two presented represent a simple single point analysis and a more detailed analysis covering the operating range of the propeller. These two approaches to the basic analysis can quickly supply answers to the most common questions regarding propeller performance, such as whether of not a given propeller is suited for a particular task and what is the estimated performance of the propeller over a complete mission. Because they are easy and quick to use these types of analysis tools are very useful in the propeller design process. This process requires a significant amount of iteration with a number of propeller geometries in order to narrow the choices to a few configurations.

The main drawback to these types of analysis is that the accuracy of their results can vary widely. For conventional flight conditions the aerodynamics are well known and these methods should produce fairly accurate results. However under situations in which the behavior of the fluid flow is influenced by factors not usually encountered in conventional flight, the accuracy and trends predicted by these methods could be quite poor. Unfortunately these nonconventional

conditions, such as low Reynolds number and high subsonic Mach number operation are characteristic of the propeller environment for the proposed high altitude low speed mission. A possible way to circumvent this problem is to utilize the detailed 2D analysis to generate airfoil performance which is representative of this unique flight regime and then use this data in conjunction with the more basic methods, such as the vortex theory code, to produce more accurate results. More on this approach is given in sections 4.1.1 and 4.2.1.

4.1.1 Vortex and Momentum Theory Analysis

An analysis capability was set up to provide a means of generating a performance map of a given propeller geometry. The analysis code, shown in appendix C, which was developed could use three separate approaches to determine the propeller performance. These methods are momentum theory, vortex theory with small angle assumptions and vortex theory.[6,7] The main difference between these methods is in how the induced velocity, w, is calculated. These analysis utilize the propeller geometry and airfoil performance characteristics to determine the propeller's performance. Therefore if the geometry and airfoil performance is known, any propeller can be analyzed. The more accurate the airfoil data the more accurate the results. This type of analysis can be used in conjunction with airfoil performance prediction codes as mentioned previously to produce a fairly accurate performance map of a given propeller design. These airfoil performance codes are discussed in section 4.2.1.

The following information on the propeller is necessary in order to estimate the performance.

- Propeller Airfoil Lift Curve Slope Including any Post Stall Data for each Radial Station
- Airfoil Maximum Lift Coefficient
- Propeller Hub Diameter
- Propeller Blade Twist as a Function of Radius
- Airfoil Thickness as a Function of Radius
- Chord Length as a Function of Radius
- Airfoil c_d versus c_l Curve for each Radial Station

With this information listed above the performance analysis can be done for both design and off design points allowing for the generation of a complete performance map of the propeller. The theory behind the analysis techniques used is well established and has been available for a number of years. All the

methods calculate the thrust coefficient c_t and the power coefficient c_p by means of the following relations.

$$c_t = (\pi / 8) \int_{xh}^{1} (J^2 + \pi^2 x^2) \sigma [c_l \cos(\phi + \alpha_i) - c_d \sin(\phi + \alpha_i)] dx \quad [4]$$

$$c_p = (\pi / 8) \int_{xh}^{1} \pi x (J^2 + \pi^2 x^2) \sigma [c_l \sin(\phi + \alpha_i) - c_d \cos(\phi + \alpha_i)] dx \quad [5]$$

Where the advance ratio, **J**, the normalized radial distance, x, and the variables σ and ϕ are represented by the following expressions.

$$J = V / (z D) \quad [6]$$

$$x = r / R \quad [7]$$

$$\sigma = (n c) / (\pi R) \quad [8]$$

$$\phi = \tan^{-1}(V / (\omega R x)) \quad [9]$$

The variables used in the above equations are defined below.

a Airfoil Lift Curve Slope

c Airfoil Chord Length

c_d Airfoil Drag Coefficient

c_l Airfoil Lift Coefficient

D Propeller Diameter

n Number of Propeller Blades

R Propeller Radius

r Local Radius of an Airfoil Station

V Free Stream Velocity

xh The nondimensional radial distance of where the hub ends and the propeller blade begins.

z Propeller Rotations per Minute (RPM)

β Propeller Pitch Angle

α_i Induced Angle of Attack

ω Rotational Velocity (radians / second)

A brief description of each of the analysis methods is given below and a copy of the computer source code is given in appendix C.

Momentum Theory: In momentum theory the propeller is approximated by a thin disc across which there is an increase in static pressure. This method does not take into account the specifics of the propeller design and therefore is limited in its accuracy. Some of the assumptions inherent to this method are that the slipstream velocity through the propeller disc is constant over the area of the disc, the pressure change is uniform over the area of the disc and the flow is assumed incompressible.

The assumptions in the momentum theory which allow for the direct calculation of the induced angle of attack, α_i, and the corresponding induced velocity are that α_i and the drag to lift ratio are very small (much less then 1). This enables the induced angle of attack to be represented by the following equation.

$$\alpha_i = 1/2 \left[\left(V / (\omega R x) + n\, c a V_r / (8x^2 V_t \pi R) \right)^2 + n\, c a V_r (\beta - \phi) / (2x^2 V_t \pi R) \right]^{0.5} - 1/2 \left(V / (\omega R x) + n\, c a V_r / (8x^2 V_t \pi R) \right) \quad [10]$$

Where the radial and tangential velocity components, V_r and V_t respectively, are given by the following expressions.

$$V_r = V_t \sqrt{(x^2 + (V/\omega R)^2)} \quad [11]$$

$$V_t = \omega R \quad [12]$$

Using the above equations and a known propeller geometry the performance of a propeller can be calculated for both design and off design points. This is done by performing the calculations at each airfoil station along the blade length. From performance data generated a complete operational map of the propeller can be made.

Vortex Theory : Vortex theory, also call strip theory analysis, can be used to determine a propellers performance for both design and off design conditions. The theory differs from momentum theory in that it takes into account 3D flow field effects on the propeller performance. This is done by calculation the losses due to the vortex generation form the induced velocity created by the propeller as lift is created. This loss is similar to the induced drag loss generated by an aircraft wing during flight. This theory differs form the momentum theory given above in how the induced velocity and corresponding induced angle of attack are

calculated. The vortex theory calculations can be simplified by assuming the induced angle of attack is small. Based on this assumption, α_i, can be calculated by the following expressions.

$$\alpha_i = 1/2 \sqrt{[(\tan(\phi) + nca / (8xF \cos(\phi))^2 + nca (\beta - \phi) / (2\pi RxF \cos(\phi))]} - 1/2 (\tan(\phi) + nca / (8xF \cos(\phi))) \quad [13]$$

Where the expression for Prandtl's tip loss factor, F, is given by the following.

$$F = 2/\pi [\cos^{-1} \exp (n (x-1) / (2 \sin (\tan^{-1} (V/\omega R))))] \quad [14]$$

To increase the accuracy of the vortex theory analysis the small angle assumption can be dropped. Without the small angle assumption used above the induced velocity must be calculated by determining its vector components. For this case the induced angle of attack is represented by the following equation.

$$\alpha_i = \tan^{-1}(w_t/w_a) - \tan^{-1}(V/\omega Rx) \quad [15]$$

Where w_t and w_a are the tangential and axial components of the induced velocity respectively. Expressions for these velocity components are given by the following equations.

$$w_a = 1/2 [\sqrt{(V^2 + 4 w_t (\omega Rx - w_t))} - V] \quad [16]$$

$$w_t = (nca / \pi R) \{ \beta - \tan^{-1}(w_t^2 /(2 w_a)) \sqrt{(1/4 (V/\omega R + \sqrt{((V / \omega R)^2 + 4w_t(x - w_t/V_t) / V_t))^2 + (x - w_t/V_t)^2}) - 8xF w_t/V_t} \quad [17]$$

The above equations for w_a and w_t must be solved iteratively. Once these values are known α_i can be calculated for each airfoil station and the overall performance of the propeller can then be determined. Due to the iterative nature of this method the computational time will be longer then for the previous methods described. In general the full vortex analysis will produce more accurate results then either the momentum theory analysis or the vortex theory analysis with small angle assumptions. The momentum theory will tend to produce more optimistic results whereas the vortex theory with small angle assumption will produce more pessimistic results then the full vortex theory analysis. Due to the speed of today's computers once the vortex theory analysis is

set up it is preferable to use this method. Figures 18 through 25 show some results generated by the computer code given in appendix C utilizing the full vortex theory analysis method. These results show the torque and thrust generated by a propeller at various operational altitudes. Each graph is done for a number of blade angle values.

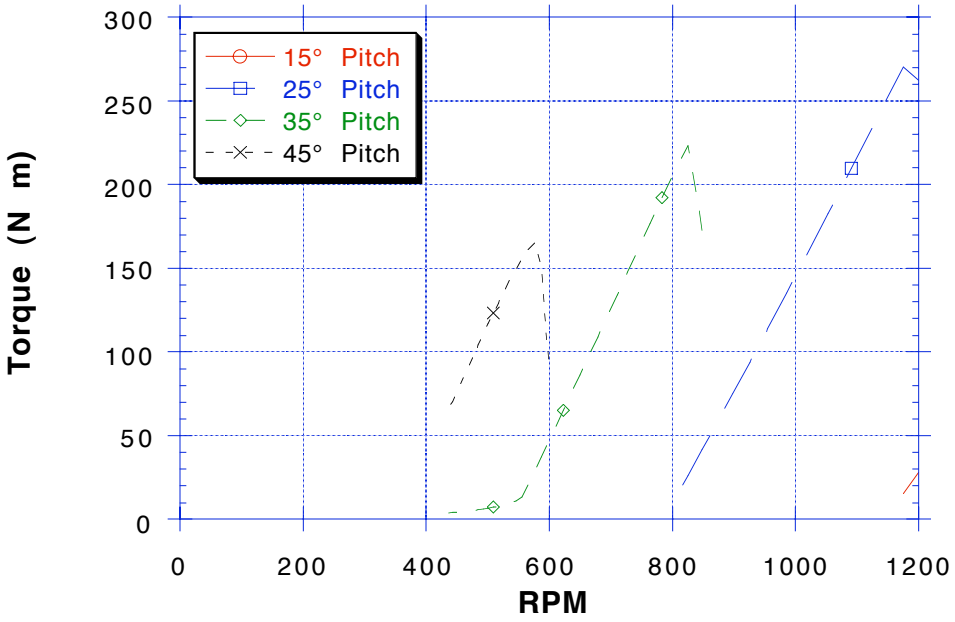

Figure 18 Torque Curves Generated with Vortex Theory Code for a 2 Bladed Propeller operating at 27 km Altitude

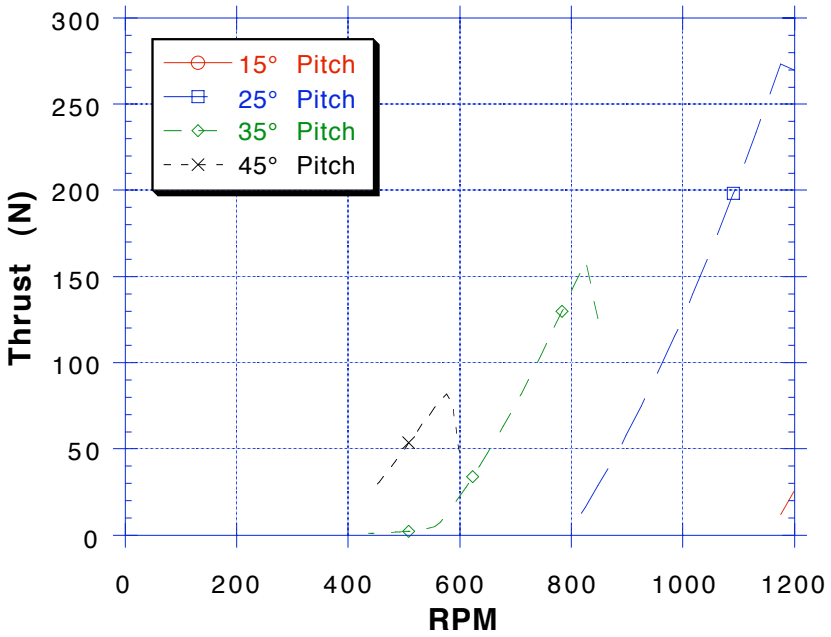

Figure 19 Thrust Curves Generated with Vortex Theory Code for a 2 Bladed Propeller operating at 27 km Altitude

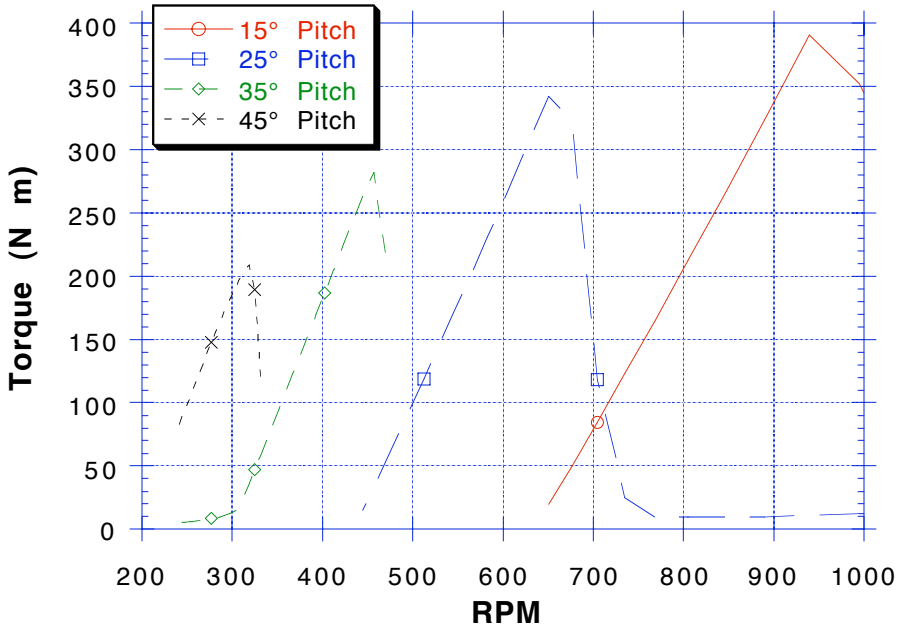

Figure 20 Torque Curves Generated with Vortex Theory Code for a 2 Bladed Propeller operating at 18 km Altitude

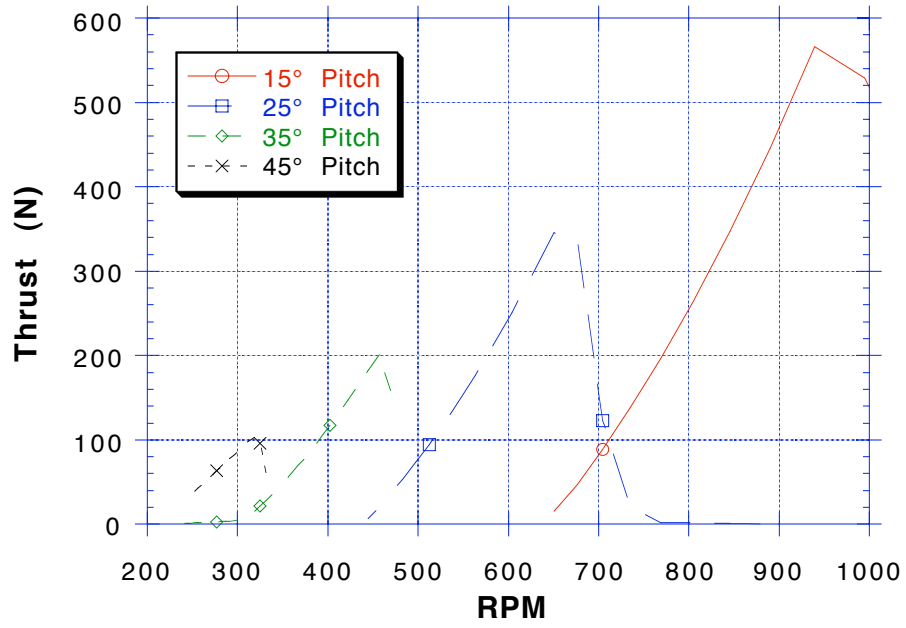

Figure 21 Thrust Curves Generated with Vortex Theory Code for a 2 Bladed Propeller operating at 18 km Altitude

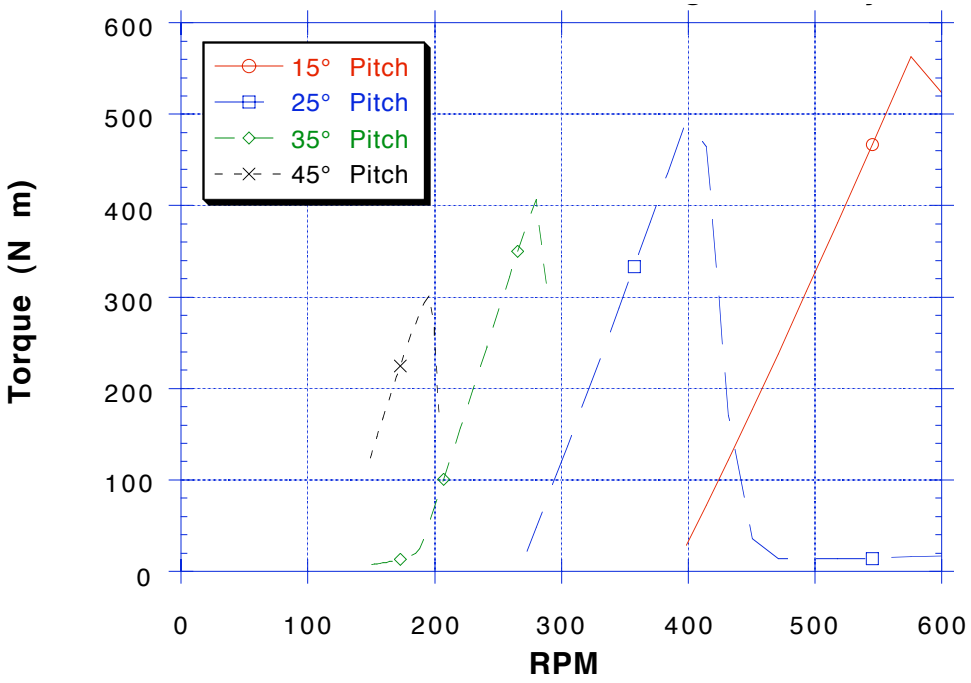

Figure 22 Torque Curves Generated with Vortex Theory Code for a 2 Bladed Propeller operating at 9 km Altitude

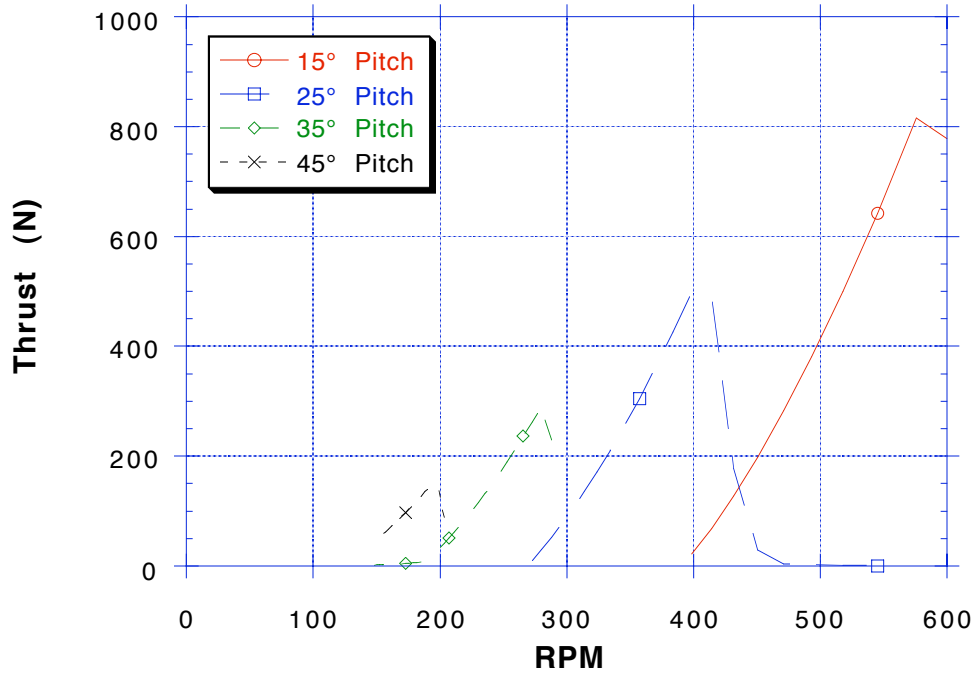

Figure 23 Thrust Curves Generated with Vortex Theory Code for a 2 Bladed Propeller operating at 9 km Altitude

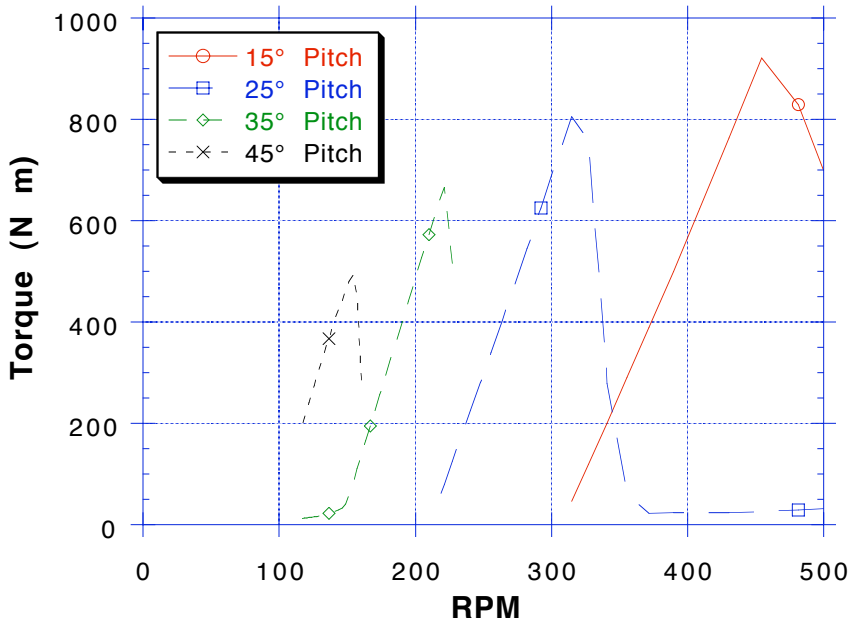

Figure 24 Torque Curves Generated with Vortex Theory Code for a 2 Bladed Propeller operating at Sea Level

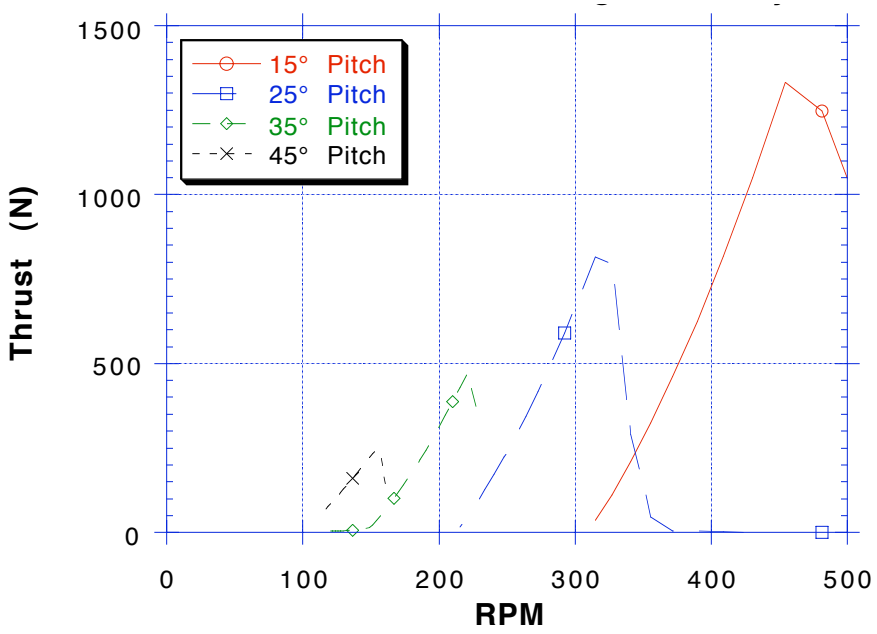

Figure 25 Thrust Curves Generated with Vortex Theory Code for a 2 Bladed Propeller operating at Sea Level

4.1.2 Spread Sheet Analysis

A simple spreadsheet analysis was set up to provide a quick estimate of the performance of a given propeller. This performance analysis utilizes on the flight conditions and basic geometry of the propeller. This analysis is based on single point propeller performance method developed by Henry V. Borst and Associates, shown in reference 7. The analysis method is derived from the premise that the three-quarters blade location can be assumed to represent the performance of the entire blade. The analysis also takes into account effects due to low Reynolds number operation.

A number of quantities related to the flight environment and propeller design performance and geometry must be inputted in order to begin the analysis. These quantities are listed below.

- Shaft Power out of the Engine (hp)
- Propeller RPM (z)
- Flight Altitude
- Forward Velocity (V_o)
- Average Local Velocity (V)
- Propeller Diameter (D)
- Number of Propeller Blades (n)
- Blade Activity Factor (AF)
- Blade Design Lift Coefficient (C_l)
- Propeller Airfoil Lift To Drag Ratio (L/D)

The average local velocity (V) is the free stream velocity at the propeller location. This is usually slightly less the the forward velocity due to interference effects between the aircraft body and the free stream. Based on the desired flight altitude the ratio of atmospheric density at altitude to that at sea level (σ) can be determined as well as the atmospheric viscosity (ν).

The value of blade activity factor is a nondimensional number which represents the solidity or geometrical shape of the blade. It is a way of classifying the overall blade shape and is useful for comparing two separate propellers whose applications may be very different. The expression for activity factor is as follows:

$$AF = (100{,}000/16) \int_0^1 (c(x) / D)\, x^3\, dx \qquad [18]$$

Where c is the chord chord length as a function of the radius of the blade station of interest divided by the total radius of the propeller (x). D is the blade diameter.

$$x = r / R \qquad [19]$$

For a constant chord propeller the activity factor reduces to the following expression.

$$AF = 1562.5\ c(x) / D \qquad [20]$$

Using the values of the quantities listed above an estimate of the propeller efficiency can be made. The following is an outline of the calculations which are done in order to determine this efficiency.

- Calculate the pressure coefficient (c_p) .

$$c_p = \frac{(0.0005)\ (hp)}{\sigma\ (z/1000)^3\ (D/10)^5} \qquad [21]$$

- Calculate the advance ratio based on the local velocity (**J**).

$$\mathbf{J} = \frac{60\ V}{z\ D} \qquad [22]$$

Based on c_p , **J** and n, the induced efficiency η_i can be found from figures 26, 27 and 28.

- Calculate the Lift to Drag angle γ.

$$\gamma = \tan^{-1}\ (1 / (L/D)) \qquad [23]$$

- Calculate the blade operating Reynolds number (Re)

$$Re = (\nu_{sl} / \nu)\ 4\ AF\ D\ (V^2 + (0.75\ \pi\ z\ D / 60)^2)^{\cdot 5} \qquad [24]$$

- Calculate the apparent air incident angle θ_o .

$$\theta_o = \mathrm{Tan}^{-1}\ (0.4244 * \mathbf{J}) \qquad [25]$$

- Calculate the actual air incident angle ϕ.

$$\theta = \mathrm{Tan}^{-1}\ (\mathrm{Tan}(\ \theta_o.) / \eta_i\ ) \qquad [26]$$

- Calculate the estimated propeller efficiency η.

$$\eta = \tan\ (\theta_o) / \tan\ (\theta + \gamma) \qquad [27]$$

If the calculated Reynolds number is less the 500,000 then an adjustment to the value of γ needs to be made to take into account low Reynolds number effects. This adjustment is given by the following steps.

- Calculate the operating lift coefficient C_{lo}.

$$C_{lo} = 0.027343 + 0.9934\,(L_1) - 0.152\,(L_2)^2 \qquad [28]$$

where L_1 and L_2 are given by:

$$L_1 = 400\,c_p / (n\ AF) \qquad [29]$$

$$L_2 = 4000\,c_p\,\mathrm{Sin}(\theta) / (n\ AF\ J^2) \qquad [30]$$

Using the value of C_{lo} and the design C_l the value of the gamma correction factor (γ_{cf}) due to low Reynolds number effects can be found from figure 29.

- Calculate the corrected gamma value γ_{cr}.

$$\gamma_{cr} = \gamma\,\gamma cf \qquad [31]$$

This corrected value, γ_{cr}, is used in place of γ in equation 27 to calculate the propeller efficiency.

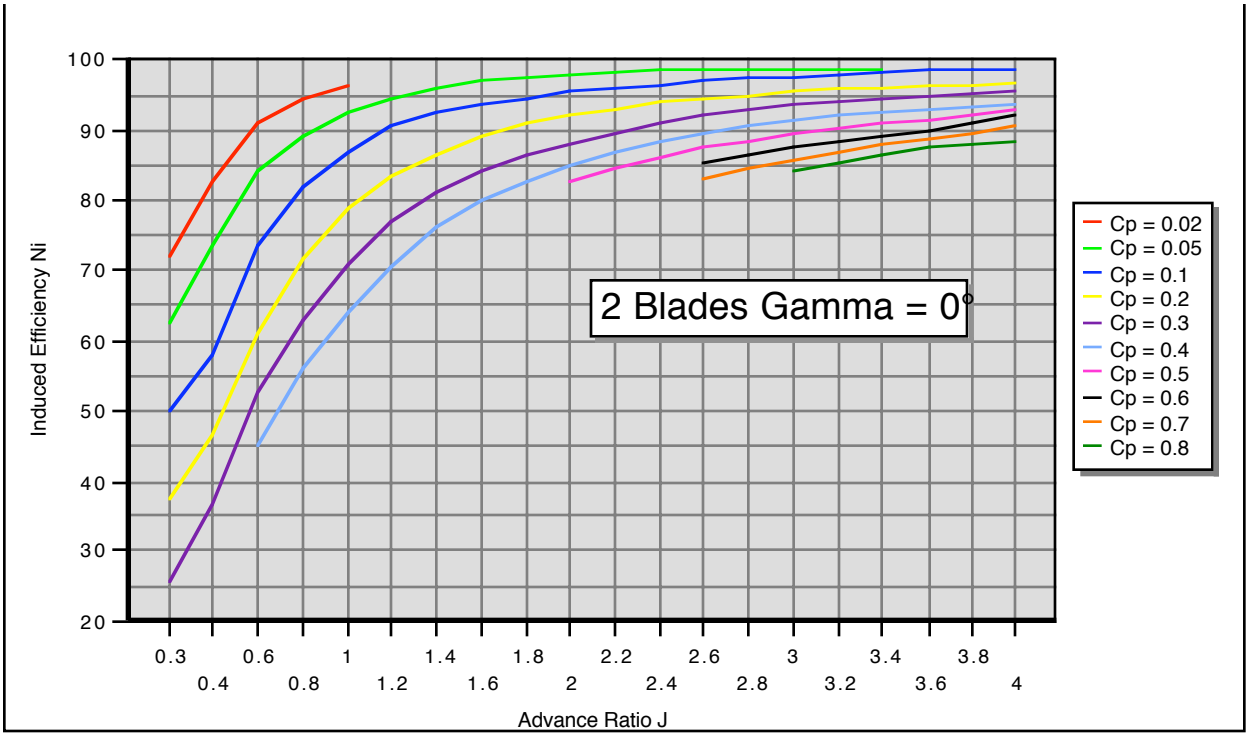

Figure 26 Induced Efficiency Curves for 2 Bladed Propeller

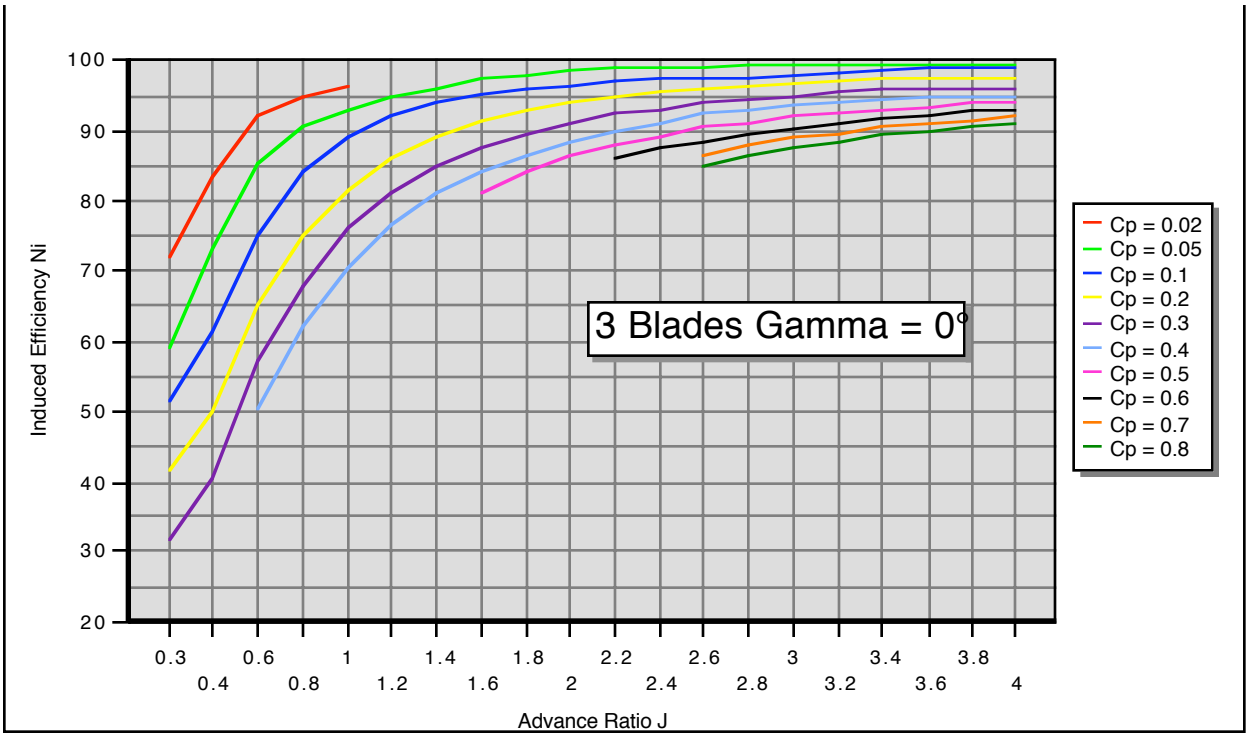

Figure 27 Induced Efficiency Curves for 3 Bladed Propellers

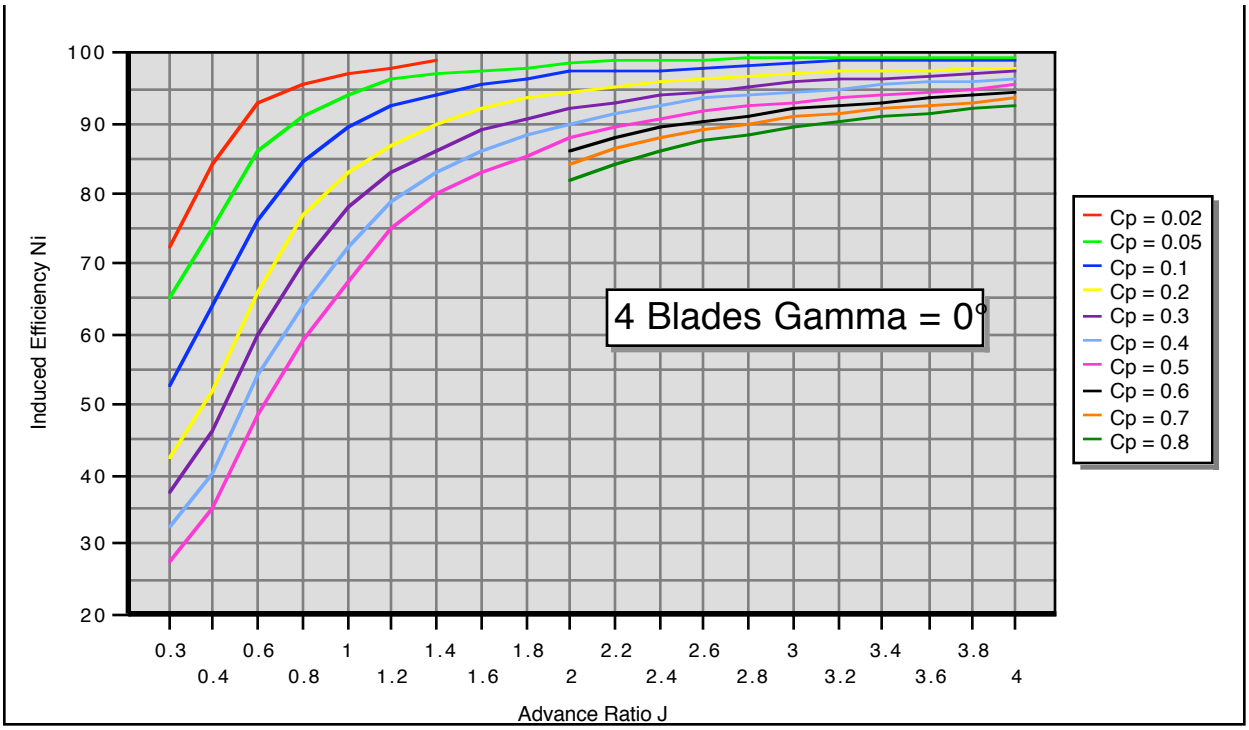

Figure 28 Induced Efficiency Curves for 4 Bladed Propeller

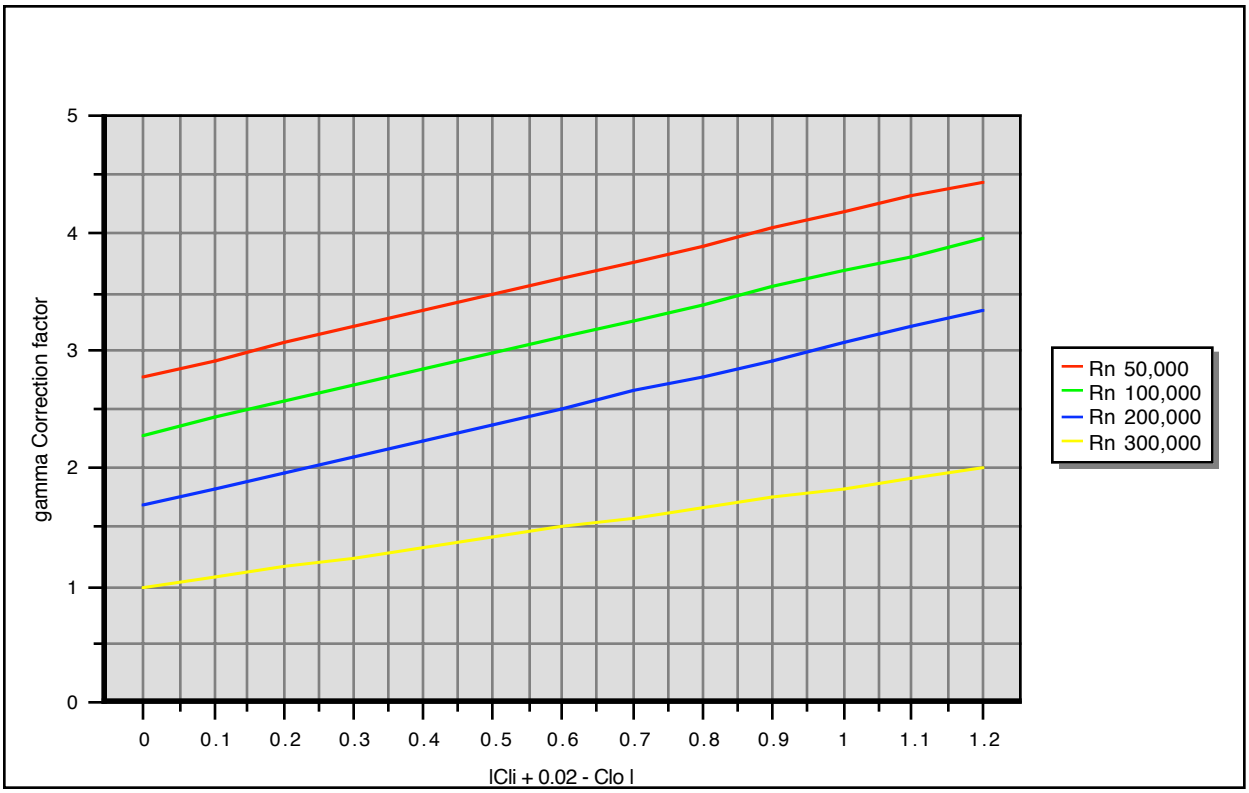

Figure 29 Gamma Correction Factor for Low Reynolds Number Effects

4.2 Detailed Analysis

The detailed propeller analysis and approach is to utilize computer modeling to analyze a propeller and estimate its performance. A number of computer codes are available of this type of analysis. However they differ greatly in their accuracy, ease of use and applicability to the high altitude flight environment required for the ERAST aircraft.

There are two main approaches to the computer code analysis being considered. The first method is to do a 2D airfoil analysis in the low Reynolds number high subsonic Mach number regime. This analysis will be used to produce airfoil performance data over a range of angles of attack. The airfoil data can then be used in conjunction with a vortex or strip theory propeller analysis code to determine the performance of a propeller based on this airfoil data. This method would be useful in producing a rough performance estimate for a propeller over its complete operating range. The main drawback to this type of analysis is that flowfield interactions between various types of aerodynamic phenomena, such as boundary layer growth and shock wave formation are not well represented. This can affect the accuracy of the predicted propeller performance especially in the low Reynolds number, high subsonic Mach number regime common to high altitude propellers. In order to account for these

types of interactions a computer code capable of analyzing a full 3D flow field is required. A full 3D analysis is done by obtaining the geometry of the propeller under loaded conditions and producing a full 3 dimensional grid around the propeller shape. This grid can take into account any aircraft components near the propeller which are close enough to have an effect on the flow field around the propeller. This distance is usually estimated as 1 propeller diameter. This grid is then used by the analysis code to estimate the propeller performance. This 3D analysis method would provide an accurate performance prediction of a given propeller under the flight conditions, assuming that the correct grid geometry and accurate propeller shape is used.

There are some obstacles to using the computer modeling approach given above to directly determine the propeller performance within the low Reynolds number high subsonic Mach number regime of interest. These are listed below.

* There has been very little propeller analysis work done in this regime. Through the extensive literature search that was performed no useful experimental data for either an airfoil or propeller within this regime has been found. Therefore there is no way to validate the computer codes to be assured that the results generated for this type of flight regime would be accurate.

* Based on the design characteristics of the Condor propeller , the only combustion engine driven propeller designed and flown to high altitudes, a high altitude propeller will most likely be light weight and large. Because of these characteristics the propeller blade will tend to flex under loading conditions more then is normally seen for conventional propellers. This means that the actual operational geometry of the propeller will be different then that of the propeller under no load conditions. Therefore in order to use a computer code to get an accurate estimate of the propeller's performance the loaded or "hot" geometry needs to be obtained. This is possible by using various structural analysis codes if the complete structural makeup of the propeller is known as well as its aerodynamic loading. Therefore in order for a truly accurate 3D analysis to be performed on a given propeller design a structural analysis would need to be performed in conjunction with the aerodynamic analysis.

4.2.1 2D Airfoil Analysis

One possible test of the 2D propeller codes is to use them to analyze the geometry of the Condor propeller. Details on the Condor propeller are given in section 3.1. The Condor propeller presently is the best choice for comparing the capabilities of each of these computer codes since this is the only propeller which has been powered by an internal combustion engine and is proven to be capable of providing thrust at altitudes up to 20 km (≈ 67,000 ft). Also due to the CNC mapping of the propeller the geometry is accurately known. It would be a good test to see how the results from each of these 2D propeller codes compared to each other as well as to the propeller performance map generated by Hartzell, the propeller manufacture. To accomplish this the codes would be run to generate

drag versus lift curves for the various propeller geometries of the Condor propeller. Lift to drag data would be generated over a range of angle's of attack and Reynolds number combinations. This data would be curve fit any incorporated into a vortex theory code, details of which are given in section 4.1.1. This vortex theory code would then be used to generate a performance map of the propeller for a range of advance ratios (J). By comparing the resulting performance maps and lift to drag data the differences in the accuracy of the codes could be assessed. It should be noted however that the performance map generated by Hartzell was not produced by experimental testing. It was generated by an in house computer code. Therefore it's accuracy is also questionable. As discussed in section 3.1, Boeing did perform some testing of the propeller during flight. The results although not conclusive did suggest that the Hartzell performance data was not entirely accurate over the complete flight regime tested.

The advantages of using a vortex or strip theory analysis over a full 3D analysis is speed. During the design process for a propeller the need to change the propeller characteristics can occur frequently. Using a strip theory code with accurate airfoil data will allow the calculation of propeller performance at many off design points. This ability to calculate the propeller performance quickly allows for the creation of a complete propeller map, which is essential in determining the applicability of a given propeller to a particular mission.

The following are a list of computer codes which are capable of performing a detailed 2 dimensional performance analysis of an airfoil. The basic principle of operation of each computer code is given as well as its capabilities and present status of operation for this high altitude propeller analysis application.

Eppler airfoil analysis code:[8] This code uses a conformal mapping method to design airfoils for a given velocity distribution. A panel method and boundary layer analysis are used to analyze the potential flow about an airfoil in order to estimate it's performance. The code was written specifically for low Reynolds number airfoil analysis. This computer code is written in FORTRAN IV and is available through COSMIC. It was written in the early 80's by Richard Eppler of the University of Stuttgart and Dan Somers of NASA Langley Research Center. The original code was written for a Control Data 6600 computer system. It has some subroutine calls specifically for this type of computer. These calls are mainly for printing and plotting functions.

Due, probably, to the age of this computer code there was difficulty in obtaining it on a computer disc. Therefore the source code was scanned and or hand typed in from the copy contained in the NASA report on the code given in reference 8. The code was ported to a Silicon Graphics computer. Since some of the calls for the code were not applicable to this type of computer certain modifications had to be made to the computer code. The printing and plotting algorithms were removed and the input file format was changed. The code was set up to use two separate input files one describing the type of analysis to be performed and the other providing the airfoil geometry to be analyzed. A copy to

these input files are given in Appendix D. The code was compiled using certain options to make it compatible with the FORTRAN 77 compiler which was used. One of the more important options was *-static.* This option stores local variables to a static location and sets their initial value to zero. This was a standard option for compilers on the older mainframe computers, however for modern day machines it must be specifically designated. Without this option the code will run intermittently and crash at inconsistent points of operation making it very difficult to trace down the problem. The code was successfully compiled and run with the input data given in the appendix. The airfoil geometry given was for a FX63-137B airfoil. The performance analysis was specified to be done for airfoil angles of attack of 2° to 10° in increments of 2° and for various Reynolds numbers form 1,000,000 to 150,000. At the time of this writing the results form this initial test case indicate that the code is not yet operating correctly. It is believed that with some additional effort the code could be rendered operational.

ADPAC (Advanced Ducted Propfan Analysis Codes) [9] Since this code's main application is for 3D flowfield analysis a complete description of its operation and characteristics are given under section 4.2.2, 3-D Propeller Analysis. Even though the main application for this code is 3D flowfield analysis it is also capable of performing a 2D analysis on an airfoil. This 2D analysis could be used to determine its performance over a range of angles of attack. The results could then be used in conjunction with a vortex theory or some other propeller analysis code to estimate the propeller's performance. This type of analysis was performed by Lisa Koch for her master's thesis[10]. In this thesis ADPAC was used to generate 2D section performance predictions for Reynolds numbers of 60,000 and 100,000 and Mach numbers ranging from 0.45 to 0.75. A 3D analysis was also performed, using ADPAC, and compared to the strip theory analysis using the 2D airfoil data. The results stated that the difference in propeller efficiency between the two methods was 1.5% and the predicted thrust, power and torque coefficients were 5% different. Based on the results presented in this thesis, there is not a significant difference between the 2D and 3D ADPAC results. This indicates that the use of this code in conjunction with a vortex theory or other strip theory analysis code can be considered a viable alternative to a full 3D analysis. Therefore if the code is proven, through experimental testing, to be capable of producing accurate results for 2D airfoil sections within the low Reynolds number, high subsonic Mach number regime, then it can be inferred that it should be accurate for 3D modeling as well. More details on the code validation and 2D airfoil experimental testing are given in sections 5.1 and 5.2.

The main drawback to using ADPAC for the 2D analysis is that it is not designed for the type of repetitive analysis required to produce the desired amount of airfoil data. The operation of the code in this manner would take considerable time and effort to produce enough airfoil data to generate a full propeller performance map.

XFoil Code [11] This computer code is written in FORTRAN 77 and was developed at the Massachusetts Institute of Technology. It is for the design and

analysis of subsonic airfoils. It is capable of performing a viscous or inviscid analysis of a given airfoil. It accounts for boundary layer transition both forced and natural, boundary layer separation bubble formation and flow separation. Details of the methods used by the code for its analysis are given in references 12 and 13. The inviscid analysis is a linear-vorticity panel method, similar to that used in the Eppler airfoil analysis code. A Karman-Tsien compressibility correction is used to allow for good compressible flow predictions up to a sonic condition. For the viscous analysis the inviscous solution is used in conjunction with the viscous equations and is solved by a full - Newton method of analysis. This code been acquired and its operation and applicability to this propeller analysis has to date not been performed. The results of this code have never been validated for the low Reynolds number /High Mach number regime which is of interest to high altitude propeller analysis. In order to determine the applicability and accuracy of this code it would need to be validated against experimental data within the regime of interest.

MCARFA This is a multi component 2D viscous airfoil analysis code. It was written at the NASA Langley research center in the late 1970's. To date the operation and applicability of this code to the high altitude propeller analysis problem has not yet been done. Detailed information on the operation of the code has not yet been acquired. Once more information is available the applicability of this code will become evident. In any regard the code will still need to be validated in order to have confidence in its results for low Reynolds number high Mach number applications.

MSES[14] This is a multi element airfoil design and analysis code. It was written at MIT in the mid 1990's and continues to be updated. It actually consists of a number of separate computer codes which are used in conjunction with each other depending on the type of analysis or design desired. These codes perform preprocessing, analysis and post processing tasks. The codes used for preprocessing are AIRSET and MSET.

AIRSET[15] is an interactive program which allows for the manipulation of the airfoil configuration. This includes tasks such as moving a flap, modifying the shape of the airfoil, rotation and translation of the airfoil and scaling of the airfoil.

MSET generates the grid and initializes the flowfield. This is an interactive program which allows for the generation and manipulation of the flowfield grid.

Once this preprocessing is completed the grid generated is then used in the MSES flow solver code. This code solves the viscous Euler flowfield equations for the flow around the airfoil. The number of iterations can be specified and after each iteration is completed the change in certain parameters which give an indication as to the convergence of the solution for the given airfoil is displayed. If it is desired to examine a number of angles of attack a specialized version of MSES, called MPOLAR, is used. Other variants of MSES include MPOLARC and MPOLARM.

MPOLAR will perform the same analysis as MSES over a specified range of angles of attack of the airfoil. It is a much less time consuming and easier way to produce data over a range of angles of attack then setting up and running the cases individually. This type of comprehensive angle of attack analysis is necessary for incorporating airfoil performance into a propeller analysis code.

MPOLARC is the same as MPOLAR except it uses the lift coefficient of the airfoil as its convergence criteria.

MPOLARM steps through a range of Mach numbers instead of angles of attack for the given airfoil geometry.

MSIS is a version of MSES which assumes an isentropic condition everywhere. This code runs faster and can calculate flows for extremely small freestream Mach numbers. There is a version of this code which performs a similar function as MPOLAR, it is called MPOLIS.

Once data is generated it can be plotted using the code PPLOT or MXPLOT. Data such as the c_l vs c_d and angle of attack vs c_l can be plotted. MPLOT is a program which is used to display the MSES solution data at any time.

After an analysis is completed MEDP can be used to modify the resulting data and redesign the airfoil to match the edited output file.

The combination of computer codes described above, commonly referred to as just MSES, is the newest and most detailed available for performing 2D airfoil analysis. This code is capable of handling both low Reynolds number and high subsonic Mach number airflows. However, as with the previous codes since no data exists for an airfoil experiencing both these flow regimes simultaneously, validation still needs to be done in order to verify the code's ability to model an airfoil under these conditions. Due to its operational characteristics and capabilities the MSES collection of codes is probably the best selection for 2D propeller performance analysis. Since this code was recently received, at the time of this writing, there has been no airfoil and subsequent propeller analysis performed to date utilizing this code.

4.2.2 3-D Propeller Analysis

A 3D fluid flow analysis of a propeller is an intricate time consuming process. This type of analysis is best suited for examining a single performance point of the propeller or examining how external structures, such as the propeller cowling or heat exchanger inlet affect the propeller's performance. The ability to completely model the flowfield around the propeller is a very powerful tool in understanding the intricacies of the propellers operation and optimizing the design. Once confidence is gained, either through validation or some other inferred means, in the compute codes ability to accurately model the desired propeller and conditions, various configurations can be examined at a fraction of

the cost of an experimental analysis. This is the main advantage of the 3D propeller analysis. Also for certain problems a detailed experimental analysis may not be possible. This may be the case with a high altitude propeller. Due to the size and flight conditions of these types of propellers there may not be an experimental facility which is capable of performing the experiment. Therefore if it is desired to have information on the complete propellers performance including interactions with the surrounding airframe structure the 3D analysis codes may be the only solution. The following are two computer codes which are capable of performing a detailed performance analysis of a propeller.

The basic principle of operation of each computer code is given as well as its capabilities and present status of operation for this high altitude propeller analysis application.

ADPAC (Advanced Ducted Propfan Analysis Codes):[9] This is a 3D Euler / Navier Stokes analysis code. The program utilizes a finite-volume, time marching numerical procedure in conjunction with a grid system segmented into multiple blocks which allows the simulation to be capable of modeling complex configurations. The code was written by Allison Engine Company for the aerodynamic and heat transfer analysis of modern turbomachinery flow configurations. Although the main development goal of this code was the analysis of steady and unsteady aerodynamics of high-bypass ducted fans, it is capable of modeling other complicated flow configurations as well. Because of the flexibility in applying this code to various problems it was considered a candidate for analyzing the flowfield of a high altitude propeller. Some of the code's features such as the ability of using multiple grid blocks and having a full three dimensional Navier-Stokes compressible flow analysis were thought to be very useful in analyzing a propeller in which the boundary layer growth and shock wave interactions are very important.

The operation of this computer code is broken into three segments. Initially an adequate gird of the propeller's geometry must be generated. This requires the use of a separate grid generation code. The one which was initially chosen for this analysis was a program called C-H Grid. Others considered were PMESH [16] and TIGG 3-D [17]. The choice to use CH Gird was made based on the recommendation of the fluid analysis group at the NASA Lewis Research Center.

The only high altitude propeller geometry available at the time the ADPAC code was being evaluated was the propeller designed for the Perseus A aircraft. This propeller had not previously flown but had been designed to achieve an altitude of 24.3 km (80,000 ft). The formatting of the Perseus propeller geometry data was not compatible with the input required by the grid generator CH Grid. So a separate data processing code had to be written which would put the data into a form which CH Grid could read. This data input problem is common among must grid generators. Each has its own particular method for reading in the airfoil data for the propeller. And since the geometry of the propeller is

usually fairly complex, including twist, taper and offset of the chord center to the propeller center line, the reordering of the propeller geometry data can be fairly complex. A copy of the source code which was used to convert the Perseus propeller data to a from usable by the gird generator CH Grid is given in appendix E and the reordered input is given in appendix F. Once the data is in the correct format it can then be used to generate a grid around the propeller shape. This gird is then used by the ADPAC code which solves the flowfield around this grid. Once a sufficient number of iterations necessary to produce the desired accuracy has been run, the output is used in conjunction with a number of post processing codes. These post processing codes allow for plotting and flow visualization of the output. In order to establish the capability to use the ADPAC code for propeller analysis a silicon graphics workstation was purchased. This type of workstation was chosen because it was similar to the type which was used by the fluid dynamics group at NASA Lewis who had previously been using the code. The grid generator and post processing codes they had been using were specific to the SGI platform. Therefore it was decided to use a similar type of computer platform in order to take advantage of their experience and established setup in running the ADPAC code.

The turbo machinery fluid dynamics department at NASA Lewis, who had originally recommended the use of the ADAPC code, began to investigate its capabilities regarding the performance analysis of a high altitude propeller. Recently they had voiced some concern over the ability of this code to be used for this type of analysis. The consensus with this code is that in order to have confidence in its results it would need to be validated with experimental data in the low Reynolds number high subsonic Mach number regime in which a high altitude propeller will operate.

Future work should continue on using the ADPAC code if validation can be accomplished or if agreement on its analysis accuracy can be established. There is the possibility of using it for 2D airfoil analysis which is discussed in section 4.2.1.

XRotor This code, written at MIT, is used for the design and analysis of propellers. It operates using lifting line theory allowing lift and drag profiles to be specified for the airfoil sections. It calculates the induced velocities by numerically solving the potential flowfield about the propeller including the vortex sheet wake. The code also includes a non-linear beam blade structural model. This model is useful for the complete design of a propeller.

This propeller code has been used extensively for the design of low Reynolds number propellers. This is the code which was used to design the propeller for the Perseus series of aircraft. However, there has been no validation either experimental or in flight conditions of this codes accuracy. Presently the acquisition of this code is being looked into.

5. Experimental Approach

Experimental tests can be done in two ways depending on the type of data needed, these are a 2D airfoil test or a complete 3D propeller test. The results of the 2D airfoil test could be used for the validation of computer analysis codes, such as those listed in section 4.2.1 or to provide airfoil data for a propeller code such as the vortex theory code listed in section 4.1.1. A complete 3D propeller test would produce propeller performance results directly as well as data for computer code validation. One of the main obstacle to the testing approach is finding a facility or platform capable of performing the test and providing sufficient results to warrant the cost. The difficulty in performing this type of experiment is due mainly to the ability to generate the low Reynolds number high subsonic Mach number flow field. Because of this flight regime an extremely low turbulence flow stream required. The low turbulence is necessary because during actual flight in a free stream there will be laminar flow over the propeller airfoil sections. Laminar flow will tend to separate from the surface of the airfoil thereby significantly reducing the propellers performance. Whereas turbulent flow will tend to adhere to the surface longer increasing performance. If the flow stream during the testing is turbulent the results generated for a given propeller or airfoil may be overly optimistic and not representative of the actual flight performance. Therefore this type of experimentation requires a unique wind tunnel facility which can meet all of these requirements or a novel approach to the testing such an an atmospheric drop test of high altitude glider test.

5.1 Computer Code Validation

To date there has been very little work done on low Reynolds number , high subsonic Mach number aerodynamics. This is due primarily to the fact that there has not been a mission which has required the operation of an airfoil within this regime. However, with the recent interest in high altitude low speed flight for atmospheric research, the need to operate within this regime is evident. This type of flight requires the use of propellers in order to generate sufficient thrust to stay aloft at the low flight speeds. Due to the low air density the size of the propeller is large compared to a conventional aircraft's propeller and the operational Reynolds numbers are low. With a large propeller the tip speed can become significant even at a fairly low RPM. Therefore, in order to generate sufficient thrust to keep the aircraft aloft the propeller will most likely need to operate with tip speeds near the speed of sound. And since the majority of a propellers thrust is generated in the outer third of the blade the operation of the propellers airfoil within this low Reynolds number high subsonic Mach number environment is critical to the propeller's performance.

Because of this unique flight requirement there is a need to design and analyze airfoils and propellers which can efficiently operate within this regime. However, because there has not been a need to operate within this regime in the past little experimental data exists and none of the presently available computer codes have been validated for this flight regime. Even with the sophistication of

some of today's newer airfoil analysis codes there is still some concern over their results relating to airfoil performance within this regime. One of the main aspects of low Reynolds number flow is the boundary layer characteristics. These include formation, growth, transition and separation. A transonic flow can have significant effects on these boundary layer characteristics, due to pressure gradient and shock formation. Because of the potential interaction of both of these flow regimes unexpected results can be produced and the ability of the computer analysis to accurately account for this interaction may be difficult.

Therefore in order for any of these computer codes to be used with full confidence in their results an experimental program should be undertaken to produce data in the critical low Reynolds number, high subsonic Mach number regime to validate the codes. There is a chance that once experimental data is generated it will be determined that a given code can not produce results accurate enough to be useful in predicting propeller performance.

5.2 2D Airfoil Testing

The main objective of the 2D airfoil testing is to obtain the airfoil aerodynamic performance over a range of operating conditions. The performance of the airfoil can be determined by the ability to measure the following quantities:

- The measurement of the lift and drag of the airfoil. These quantities can be determined by pressure measurements, both static and differential over the upper and lower surfaces of the wing. Measurements would need to be taken at a number of locations form the leading to the trailing edge of the airfoil. The sensors would not be evenly spaced. Areas of greater interest, such as the leading edge and maximum chord thickness location would have a higher density of sensors. It is estimated that the total amount of pressure sensors needed would be on the order of 50 to 100, depending of the airfoil's specific shape, in order to get an accurate measurement of the airfoils performance.

- The measurement of the boundary layer state. This state indicates the type of boundary layer which exists at a given point on the airfoil at a given time. The types of boundary layer states and other boundary layer conditions which would be of interest include, laminar, turbulent, laminar separation, turbulent separation, the formation of a separation bubble, turbulent reattachment of the separation bubble and any instability waves which may exist with the formation of the separation bubble. This type of measurement could be performed with a hot film or hot wire anemometer. The anemometers would need to be positioned at various chord stations along the upper and lower surface of the airfoil. They would need to be positioned close to the airfoil's surface in order to be within the boundary layer region. It is estimated that on the order of 50 anemometers (depending on the specific airfoil shape) would be needed in order to accurately determine the boundary layer's state. These sensors could be evenly spaced along the chord length.

- The measurement of the formation, location and strength of any shock waves which may form on the airfoil surface. This type of information can be obtained with the pressure measurements listed above along with temperature measurements of the air stream over the airfoil. Also if conducive to the experimental location a Schlieren photograph can be taken of the airflow to show the presence of any shock waves. Schlieren photographs indicate regions of varying density and therefore can also be used for visualization of the boundary layer.

Since in a 2D test only the aerodynamic performance of the airfoil is being tested not its structural integrity, the actual construction of the airfoil does not have to be the same as that used for the propeller, only the shapes have to be similar. The airfoil can be scaled to match a given Reynolds number and constructed of any suitable material without effecting the desired results. This allows some flexibility in the size of the test chamber used. In order to be applicable to this test the experimental facility or platform must be capable of attaining a Mach number of up to 0.9 with a Reynolds number of 200,000 or less. It must also be capable of providing very steady flow with little turbulence. One concern is that in order to use a conventional unpressured wind tunnel, with ambient air conditions and high subsonic Mach number flow, the chord size of the airfoil must be scaled down in order to match the correct Reynolds number. This would require the chord size to be prohibitively small, on the order of 1.5 cm. The ability to construct and instrument this size airfoil would be fairly difficult. Also, this small size enhances the turbulence effects requiring the tunnel to provide extremely steady airflow. Because of these concerns the use of an unpressurized wind tunnel will not be practical for this type of testing. Therefore either a suitable pressurized wind tunnel must be used or some other novel approach to performing this type of testing must be found. These issues are addressed in the following two sections which discuss the applicability of various wind tunnels and the APEX flight experiment.

5.2.1 Wind Tunnel Testing

The ability to perform a 2D airfoil experiment would go a long way in enabling the design of a high altitude propeller. The testing would need to be done under the same conditions in which the propeller would be operating, that is low Reynolds number and high subsonic Mach number. Ideally the data obtained would include lift and drag curves for a range of angles of attack and the complete pressure distribution and boundary layer determination over the upper and lower surface of the airfoil. This data could then be used to validate one or more of the 2D airfoil analysis codes, described in section 4.2.1. Once validated these codes could then be used with confidence for the analysis of other airfoil shapes within the same flight regime.

To date there has been little experimental work done in the low Reynolds number, high Mach number regime. The experiments which had been performed were done mainly for the production of flow visualization data not the

type of data needed for code validation.[18] Other experimental work involving low speed, low Reynolds number airfoil analysis is fairly plentiful. A fairly substantial compilation of experimental airfoil data at low Reynolds numbers is given in reference 19. This and other data has been used to validate some of the previously mentioned computer codes with fairly good results. However, when the Mach number increases the effects of compressible flow and the possibility of shock formations make the analysis much more difficult. Therefore even if the results of the computer analysis are fairly consistent with the low Reynolds number experimental results they would still need to be validated for the combined low Reynolds number high Mach number condition.

A summary of some of the available pressurized wind tunnels is given below.

The transonic dynamics wind tunnel at NASA Langley holds some promise for being capable of performing this 2D experimental task[20,21,22]. This wind tunnel is shown in figure 30. This is a pressure tunnel capable of being pumped down to an air density of 1/40 th of an atmosphere (.35 psia). This low pressure enables the ability to achieve the desired Reynolds number while utilizing a full scale or near full scale airfoil section. The tunnel test section is square and measures 4.9 m (16 ft) on a side.

Due to the need for extremely steady airflow within the tunnel to accurately test the airfoil sections, the tunnel turbulence level is a major concern. To date the turbulence measurements in this tunnel are limited to 1 atmosphere testing conditions. Presently the tunnel is undergoing calibration testing. Through this calibration process enough information should be gathered to determine if the tunnel is suitable for the low Reynolds number, high subsonic Mach number airfoil testing. Some equipment problems have occurred during the calibration process and the schedule of tests had slipped. Presently there is no indication as to when the turbulence testing will be performed, if at all. The possibility of using this tunnel will depend on the results of these calibration tests and due to the problems which have occurred during the calibration effort Langley may now require some additional funding to perform the turbulence testing which are require.

Figure 30 NASA Langely Transonic Wind Tunnel

Another tunnel which has potential for use is the NASA Ames 12 ft pressure wind tunnel. This tunnel was originally constructed in 1946 and has subsequently been rebuilt and came back online in 1995. The airflow is produced by a single stage axial flow fan powered by a 15,000 hp electric motor. This tunnel has a 12 ft diameter, 28.5 ft long test section which is capable of rotating on a 36 ft diameter carousel. The tunnel can achieve a Reynolds number of 0.1 to 12 million per foot of the test article by changing the pressure within the tunnel. The tunnel's operating pressure range is 2 to 90 psia. An air compressor run by a 12,000 hp motor which is capable of evacuating 50,000 cubic ft of air per minute is used to pressurize and depressurize the tunnel. The main advantage of this tunnel for low Reynolds number experimentation is that it has a very low turbulence level of $u'/U < 0.05\%$ and $v'/U < 0.2\%$. Due to the guide vane configuration the test section Mach number is continuously variable from 0.05 to 0.6. This Mach number range, however, is the main drawback to this tunnel. The maximum achievable Mach number of 0.6 is below that needed for the 2D airfoil testing. A picture of this tunnel is shown in figure 31.

Figure 31 Ames 12-Foot Pressure Wind Tunnel

The Unitary Plan Facility is located at the NASA Ames Research Center. This tunnel was placed into operation in 1956 and has been the most heavily used wind tunnel in the United States. It has an 11 ft by 11 ft transonic test section which can operate within the pressure range of 5 to 35 psia and with a Mach number range of 0.3 to 1.5. The main obstacle to this tunnels use for the 2D airfoil testing is the turbulence level. No data has yet been obtained on the actual turbulence level but it is believed that the level will not be sufficiently low enough to perform the low Reynolds number test which are needed. A diagram of the facility is shown in figure 32.

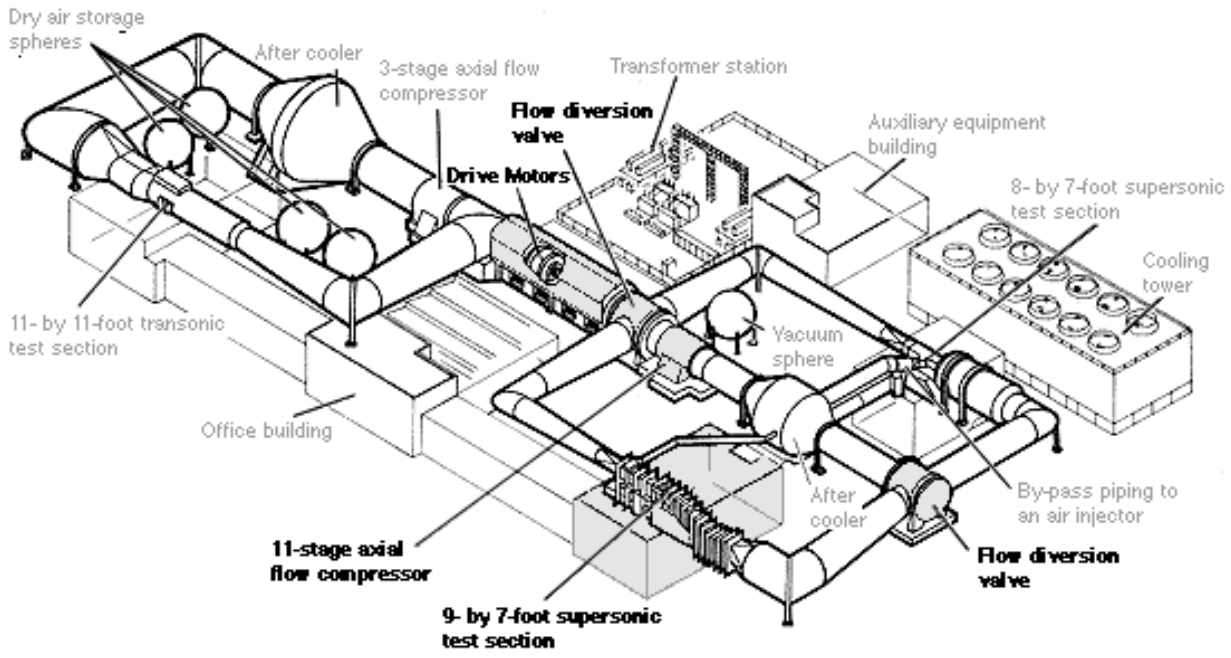

Figure 32 Unitary Plan Wind Tunnel Facility

5.2.2 APEX Flight Experiment

The APEX flight program was established at the Dryden Flight Research Center to provide a platform for testing components related to high altitude subsonic aircraft testing[23]. The main goal of the aerodynamics testing which will be performed by the APEX program is to gather data which can be used to validate computational fluid dynamic codes used in the analysis of ultrahigh altitude airfoils. The objective of the testing will be to obtain boundary layer flight test data at ultrahigh altitudes. The data collected will include the airfoil pressure distribution, drag and boundary layer data indicating what state the boundary layer is in.

The APEX flight experiment vehicle, is an unmanned glider, shown in figure 33. This glider contains all of the testing equipment, data acquisition systems, power supplies and control systems which are needed to conduct the various experiments. The APEX glider is carried to an altitude of 33.5 km (110,000 ft) by a high altitude balloon. At this altitude the glider is released and begins a controlled decent. It is during this decent phase that the experiments are performed. The airfoil aerodynamic testing will be accomplished by instrumenting a section of the APEX aircraft's wing. The initial targeted flight conditions for the airfoil testing are Mach 0.65, Cl 0.96, Re 200,000 and an angle of attack of 4°. Data can be taken over a range of altitudes. It is estimated that 4 to 6 flights will be necessary to collect the desired amount of data and to factor out any experimental error.

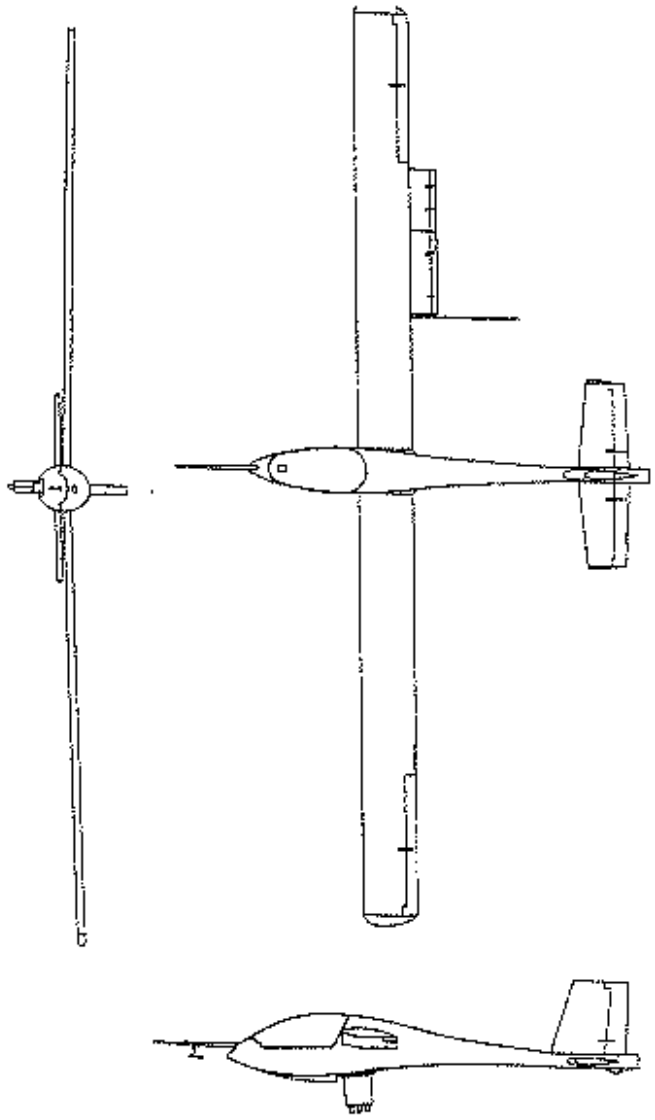

Figure 33 APEX Flight Experiment Aircraft Diagram

Presently the APEX flight experiment is still under development. The original schedule was to fly by the end of 1997. However, due to design and construction problems the schedule has slipped. The is no clear indication as to when the APEX vehicle will be operational. If and when it does become operational it should provide enough information to be able to successfully validate the computer codes listed in section 4.2.1 for 2D low Reynolds number, high subsonic Mach number applications.

5.3 3D Propeller Testing

The main objective of the full propeller testing is to directly obtain data on the propeller performance for both design and off design conditions. The factors which determine the propellers complete performance capabilities include operation at different blade angles, atmospheric densities and free stream velocities. Testing under various combinations of these factors will produce a detailed performance map of the propellers capabilities. In addition to the performance mapping the full 3D propeller testing can also be invaluable in finding and correcting any design problems associated with the propeller.

The measurement of the propeller thrust over a range of flight conditions can be accomplished in a number of ways depending on the experimental facilities. The easiest and most accurate is a direct measurement based on the force exerted by the propeller during operation. This force can be measured by devices such as a strain gage. Thrust can also be measured by monitoring the change in dynamic pressure due to the propeller operation. This method is applicable to the drop test experiment described in section 5.3.2. Or a wake survey can be performed to infer the propellers performance by measuring the change in the free stream airflow. This was the method Boeing used to estimate the CONDOR's propeller performance (see section 3.3). Ideally thrust measurements would be taken over a range of operating conditions in order to get a complete picture of the propellers performance capabilities.

Probably the most beneficial aspect of this type of testing is the ability to gather data which can be used to increase the propellers performance or correct any design problems which are found.

The propeller could be instrumented to measure the pressure field at various locations along the propeller blade. Measurements could be taken at a number of locations form the tip to the root of the blade. These measurements would indicate the performance of the airfoil sections along the length of the blade. If portions of the blade stall due to airflow separation the pressure data will record this. This type of data can give a direct indication as to why and under what conditions any changes in the propellers performance occur. In conjunction with the pressure data, strain or structural loading information can also be collected. This can be done by mounting strain gages at various locations along the propeller blade. These strain gages can indicate the state of the propeller under loaded conditions. This provides information on the twisting or flexing which can occur while the propeller is operating and under what conditions this type of motion becomes sever. Knowing the structural loading of the propeller under operation can go a long way in helping diagnose any performance problems which may occur. This type of aerodynamic and structural information can be used to either help redesign the propeller or to set limits for its operation.

The ability to perform the types of tests mentioned above will depend directly of the capabilities and operation of the proposed testing facility or device. Some possible full 3D propeller testing approaches are discussed in the following two sections.

5.3.1 Wind Tunnel Testing

The wind tunnel requirements for a full 3D propeller test are similar to those for the 2D testing. The blade Reynolds number must be low , ≈ 200,000, and therefore the wind tunnel turbulence levels must also be low. Also for reasons similar to those mentioned under the 2D wind tunnel testing, section 5.2.1, the tunnel will need to be pressurized in order to achieve the Reynolds number range with a reasonably sized test article. The required flow stream Mach number does not have to be as high as for the 2D tests. It only needs to match the flight speed of the aircraft which, for the proposed ERAST aircraft, is between Mach 0.4 to 0.6. The main obstacle for the 3D testing is the required tunnel test section size. The test section must be large enough to house a complete full size propeller. This test section requirement is very restrictive due to the large size of these high altitude propeller blades. For example the Condor propeller has a diameter of nearly 18 feet. One possible way around this size requirement is to scale the propeller and match the Reynolds number and Mach numbers to the scaled size. This approach introduces some difficult problems. Due to the proposed high altitude flight environment of these propellers, certain characteristics such as being light weight and having high aspect ratio blades, tend to be common among most designs. Because of this the actual loaded shape of the propeller is considerably different form its static shape. Therefore in order to properly scale the propeller its structure would also need to be designed so that it would deform under load in a similar manner as the full sized blade deforms under its operational loading conditions. This is difficult to account for since the actual aerodynamic loading and therefore structural deformation of the full sized blade is not known. A possible method for accomplishing this would be to measure the static deformation of a full scale propeller blade under estimated loading conditions and try to design the scaled propeller blade to proportionally match these deformations. This approach would add an additional level of complexity and expense to the testing. Also it is possible that the static loading may not truly represent the loading seen during actual operation. This could be due to some unforeseen event such as a shock wave interaction or a resonance based phenomena. Therefore there is no way to completely guarantee that the scaled propeller performance is truly characteristic of the full sized propeller.

The wind tunnels which could possibly be used to perform this 3D propeller testing are the same as those listed in section 5.2.1. Presently the wind tunnel which has been identified as having the greatest possibility of being capable of performing the full 3D propeller testing is the transonic tunnel at NASA Langley mention under the 2D testing section. The test section of this tunnel is 16 ft in diameter. This size is adequate for testing propellers on the order of 10 to 12 ft in diameter. The testing of larger diameter propellers may by influenced by wall

interaction effects. The use of this tunnel for the 3D testing is dependent on the measured turbulence level within the tunnel as discussed under the 2D testing section.

5.3.2 Atmospheric Drop Test

An alternate approach to performing a wind tunnel test on a full propeller is to test the propeller at altitude under the same operational conditions it would experience during flight. This concept was examined as a means of accomplishing the propeller testing if a suitable wind tunnel could not be found. The concept would entail using a balloon to lift a platform to high altitudes (around 100,000 ft). The platform would contain a propeller, electric motor and power source for driving the motor, most likely batteries. The balloon would raise this platform to its starting altitude, 100,000 ft, release it and then once a certain speed and altitude is attained, which is similar to that of the proposed flight aircraft , the propeller would be turned on and its thrust measured. A balloon lifting system capable of raising the platform to the required altitude can be supplied by the National Center for Atmospheric Research[24]

There are many issues which must be addressed in order to determine if the concept described above is feasible. A computer code was written to estimate the platform's characteristics, such as velocity, dynamic pressure and drag, as it descended through the atmosphere. The objective of this computer code was to determine what if any constraints there are on the platform design and to access the feasibility of the concept. This code provided the ability to investigate how changes in weight, drag coefficient, frontal area and estimated propeller thrust would affect the platform as it descended. This information was then used to determine how to best measure the propeller's thrust. A copy of the source code is given in Appendix G. Various quantities are inputted into the code to define the vehicle and set the conditions for the simulation. These quantities include:

- Initial Drop Altitude
- Overall Platform Drag Coefficient
- Total Platform Mass
- Estimated Propeller Thrust Generated
- Equivalent Flat Plate Area of the Platform
- Altitude at which the Motor is Turned On
- Duration of the Motor Operation
- Parachute Diameter

Based on the values for the inputted quantities the computer program performs a numerical integration of the forces on the platform as it descends. The instantaneous velocity of the platform is calculated at each time interval. This velocity is determined from the estimated profile drag of the platform, the changing air density and the estimated thrust generated by the propeller. This force balance is given by the following equation.

$$dv/dt = m_{tot}\, g + T - (c_d\, A\, \rho\, V^2) / 2 - D_{par} - D_{plat} \qquad [32]$$

Where m_{tot} is the total mass of the platform, g is the gravitational acceleration, T is the thrust generated by the propeller, c_d is the overall drag coefficient of the platform, A is the equivalent flat plate area of the platform, ρ is the atmospheric density and V is the instantaneous velocity of the platform. D_{par}, the parachute drag, and D_{plat}, the drag associated with an adjustable drag plate, are given by the following expressions:

$$D_{par} = 1.2\, A_p\, \rho\, V^2 / 2 \qquad [33]$$

$$D_{plat} = 1.18\, A_{plt}\, \rho\, V^2 / 2 \qquad [34]$$

Where A_p is the parachute frontal area and A_{plt} is the drag plate area. The numerical integration continues until the altitude reaches zero. The code output is a data file which contains the platform velocity and altitude as a function of time. A sample of an output file is given in appendix H.

Initially it was decided that the measurement of thrust would be done by two separate methods. This approach was taken in order to increase accuracy and add redundancy. The first method was to use a strain gauge and measure thrust based on the load applied to the platform when the propeller is turned on . The thrust measurement with a strain gage is based on the strain or force applied to the gage placed on a structural support directly in line with and behind the motor . The accuracy of this strain gage measurement is 0.1%. Therefore for a force of 445 N (100 lbf) the error in the thrust measurement would be approximately ± 0.445 N (± 0.1 lbf). The measurements from the strain gage will only be accurate when the platform has reached a steady state condition. That is the drag force balances the force due to gravity and the propeller thrust. This condition will be achieved when the dynamic pressure on the vehicle remains constant. In other words when a terminal velocity is reached.

The second method was to directly measure the dynamic pressure as the platform descended. As with the strain gage measurement a steady state condition would need to be achieved before any accurate measurements could be taken. The thrust would be inferred by measuring the steady state dynamic pressure on the platform before and after the propeller is turned on. This change in dynamic pressure could then be used to calculate the thrust of the propeller. This is given by the following expression.

$$(Q_2 - Q_1)\, c_d\, A = T \qquad [35]$$

Where Q_1 and Q_2 are the steady state dynamic pressure values before and after the propeller is operating respectively.

An analysis was then performed to determine if a terminal velocity is reached within a suitable time before and after the propeller is turned on in order to make the thrust measurements. The following assumptions are used for the analysis. The propeller is to be driven by a 75 kW (100 hp) electric motor and is estimated to produce 445 N (100 lbs) of thrust at 24.3 km (80,000 ft) with a flight velocity of Mach 0.4. The battery system used to power the electric motor is sized to provide approximately 20 to 30 seconds of operation. The overall vehicle mass is estimated to be around 250 kg (550 lbs). Based on these estimates it was determine that the vehicle would not reach a terminal velocity before dropping out of the altitude range of interest, 26 km to 20 km (85 kft to 65 kft). This result can be seen from a plot of terminal velocity versus time given in figure 34. Therefore, in order to perform the thrust measurements some other means, aside from the direct measurement of terminal velocity and strain gage methods, had to be devised.

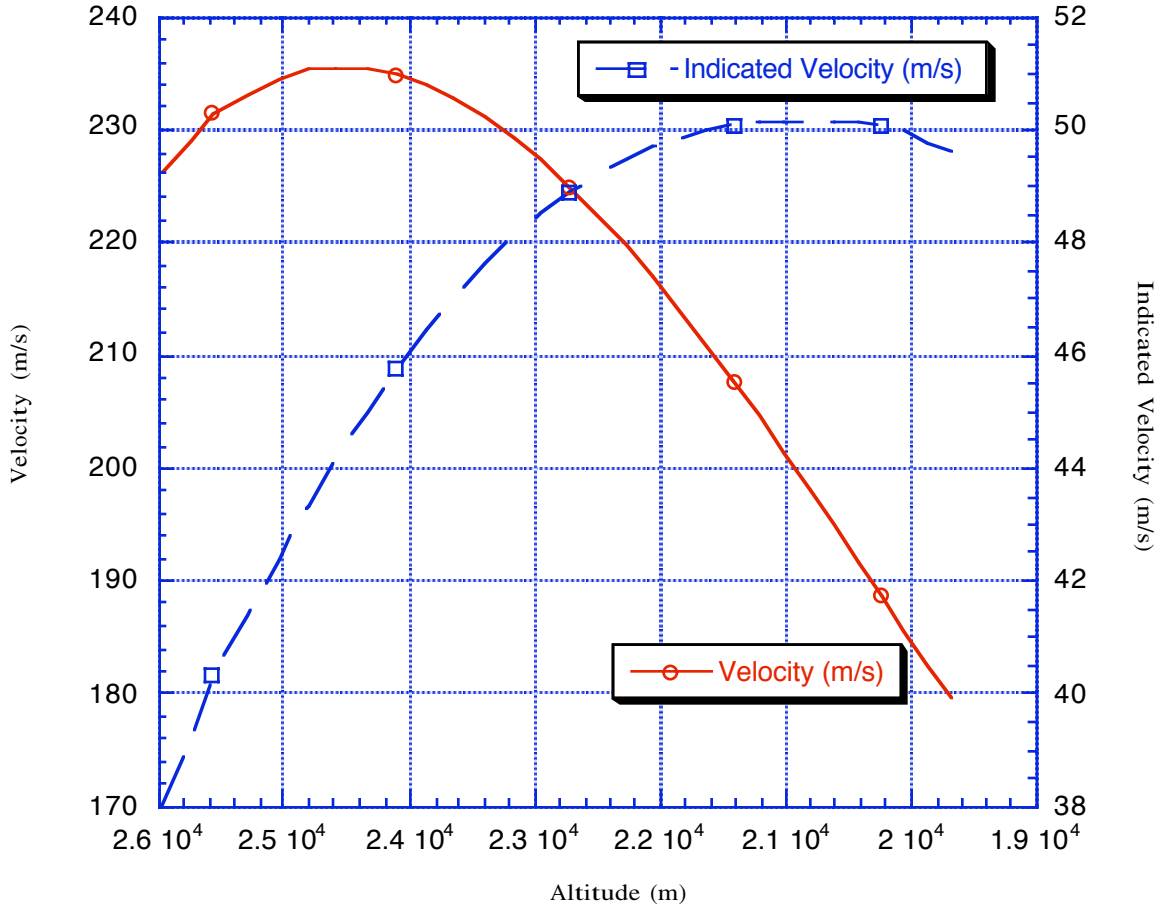

Figure 34 Platform Terminal Velocity

The alternate approach is to maintain a constant dynamic pressure on the platform by extending and retracting drag plates. This type of control system would allow the propeller thrust to be determined form the drag plate area required to maintain the desired dynamic pressure value. This relationship is given in the following relation. Where c_{dp} is the drag coefficient of the drag plate and A_p is the drag plate area.

$$Q\, c_{dp}\, A_p = T \qquad [36]$$

This drag plate concept had to be evaluated to see if this type of control system was feasible. The controls system group at NASA Lewis Research Center examined this problem and determined that with a feed back control loop sufficient response time could be achieved in order to maintain a constant dynamic pressure. In order to use this method a calibration curve is required of the platform dynamic pressure as a function of altitude. The drag plate will then be subsequently adjusted to match this dynamic pressure curve while the propeller is operating. If the control system is set to accept a propeller thrust of 445 N (100 lbf) there is approximately a 0.5 second delay in the control systems ability to adjust the drag plate once the propeller is turned on. If the initial thrust is less then expected then the time delay for the initial plate setting is greater. In the worst case when there is zero thrust the time delay is approximately 2 seconds. Once the plate area is set the control system will keep the dynamic pressure value consistent with that of the calibration curve. Therefore the error in the thrust measurement is going to be equivalent to that of the dynamic pressure measurement which is approximately 2%. Also since the control system is based on a calibration curve which is also generated by the use of a dynamic pressure sensor the total error for the thrust measurement will be approximately 4%. Therefore, based on a 445 N (100 lbf) thrust level this translates into ± 18 N (± 4 lbf) accuracy.

With this method there would be no need to wait for the platform to reach a terminal velocity and data could be taken for the majority of the time the propeller is operational. Once it was determined that the scheme was feasible from a controls standpoint, it had to be determined if sensors were available with sufficient accuracy and sampling rates to collect the data needed by the control system. The following is a list of some of the sensors available and a summary of the measurements which need to be taken.

Dynamic Pressure Sensors

Sensor Name	Operating Range	Temp Range	Repeat-ability	Response Time	Accuracy	G Sensitivity	Cost
SynSym SCXL004DN	0 to 4 " water	0 to 50 ° C	0.2% FS	500 µs	2% FS	0.6% FS/G	≈ $100.
Setra 239	0 to 5 " water	0 to 65 ° C	0.2% FS	100 ms	1%FS	0.001% FS/G	≈ $730.
Baratron 120A	0 to 5 " water	45° C	NA	NA	NA	NA	≈ $2600.

Absolute Pressure Sensors

Sensor Name	Input Power	Output	Temp Range	Pressure Range	Accuracy	Cost
Baratron Absolute Pressure Transduces 629A	± 15 VDC	0 to 10 VDC	45°C	1 atm + absolute	Standard ± 0.12% of Reading	NA

Temperature Sensor Data

Sensor Name	Altitude Range	Temp Range	Speed Range	Accuracy	Cost
Rosemount Total Temperature Sensors Model 101 Type Non-Deiced	0 to 100,000 feet	-70°C to 350° C	0 up to Mach 3	0.5% full scale	NA

Note: The rosemount temperature sensor listed above is designed for use in high altitude applications above the weather or in clear air at any altitude. They are not recommended for long-term server weather applications as deicing and antiicing provisions are not provided.

True Airspeed: The measurement of true airspeed can be accomplished by measuring the dynamic pressure, absolute pressure and the temperature.

$$Q = 0.5 \ (r) \ V^2 \qquad [37]$$

$$P = r \ R \ T \qquad [38]$$

$$V = \sqrt{(2 \ R \ T \ Q \ / \ P)} \qquad [39]$$

Therefore based on the above equation the accuracy in calculating the true

airspeed is given by the combined accuracies of the temperature sensor, absolute pressure sensor and dynamic pressure sensor. This is given by the following calculation

$$(0.98)_{\text{dynamic pressure}}(0.9988)_{\text{absolute pressure}}(.995)_{\text{temperature}} = .974$$

For a desired airspeed of approximately 0.4 Mach this translates into a true velocity measurement of ±7.5 m/s

Altitude vs Time: The measurement of pressure altitude can be accomplished by using the absolute pressure sensor described above. Altitude measurements can be taken every .005 seconds.

Based on the accuracy data given above the absolute pressure can be measured with an accuracy of approximately 99.88%. At an altitude of 24.5 km this translates into a altitude measurement of ±18 m.

Vertical Distance vs Time: This measurement is the same as measuring true airspeed. If the velocity measurement is off ± 7.5 m/s then the vertical distance, which is velocity times time, will also be off by approximately 7.5 m. This value can however compound to a much larger number. If the velocity measurement is consistently off in one direction say + 3 m/s then the error in the vertical distance measurement will be 3 meters every second. For a 30 second data window this would be a +90 meters error in the vertical distance. For the worst case of a consistent error of 7.5 meters, this translates into a 225 m total vertical distance error during the data collection period.

Dynamic Pressure: Dynamic pressure is measured using one of the dynamic pressure sensors listed above. A conservative choice from this list is the SynSym SCXL004DN. This pressure sensor has a maximum 2% error over the full scale. This translates into ± 0.08 inches of water or approximately ± 20 Pa. The time constant between measurements is approximately 0.005 seconds. Based on this sensor the error in the dynamic pressure measurement would be ±6.7 Pa.

Based on the data given above for the various sensors and measurements it was determined that sufficient accuracy can be achieved with off the shelf sensors in order to accurately measure the propeller thrust. Therefore it was determined that the possibility of using a drag plate to measure the propeller thrust was feasible.

Once it was determined that the concept of measuring the propeller performance could be accomplished with the atmospheric drop test platform, some preliminary designs were performed. The vehicles would have to be designed so that their drag, without the drag plates, would allow the vehicle to reach the desired Mach number of 0.4 at the altitude of interest. This would be done by sizing the various structural members so that they could provide necessary drag to achieve the desired velocity at the desired altitude. This sizing would need to be an iterative process taking into account the changing weight of

the platform. Another issue related to the vehicle drag is that the drag coefficients of the various components exposed to the air stream must be independent of Reynolds number. If this was not the case the overall c_d of the vehicle would change as it descended which would make calculating the propeller thrust very difficult. Shapes that have sharp corners which induce flow separation are those most likely to have c_d values independent of Reynolds number. Examples of these types of shapes are given in figure 35.

Other issues which need to be addressed in the platform design include: maintaining the correct orientation during decent, resistance to rotation during propeller operation and protection of the various components during impact.

The first design, shown in figure 36, consisted of 2 cross members approximately 9 m (30 ft) in length. These cross members would be at the top of the vehicle. The balloon used to lift the vehicle to the drop altitude would be attached at the center of these crossbars. A beam approximately 6 m (20 ft) in length would extend perpendicular form the center of the cross members. The batteries, control system and data collection system would be mounted on platforms extending from this central beam. The electric motor and propeller would be attached to the end of this beam. The drag plates would be located on the top of the vehicle attached to the two main cross members. This platform design would get its stability form having the majority of its mass located at the tip of the central boom. This would be similar to a dart. Once dropped the orientation of the platform will be maintained due to this mass distribution.

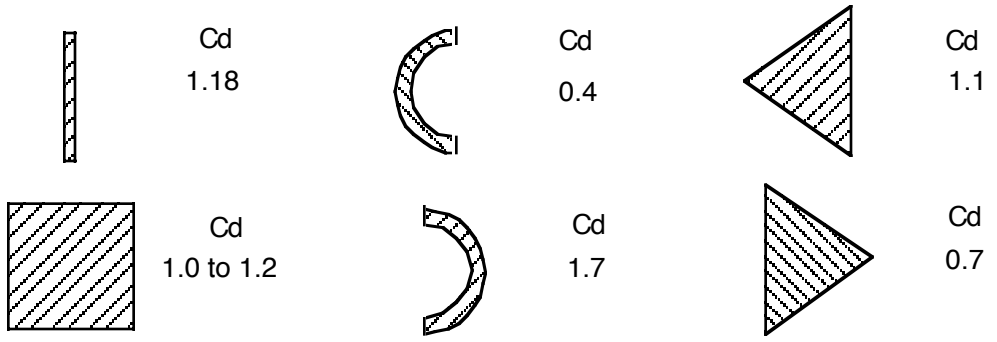

Figure 35 Shapes With c_d Independent of Reynolds Number[6]

The large cross members located at the top of the vehicle will provide substantial inertia to resist the rotation of the vehicle during propeller operation. If this proves to be insufficient then fins can be mounted off of the cross members in order to increase this rotation resistance.

The main problem associated with this design is the protection of the propeller and other components during landing. Due to their location at the bottom of the vehicle they would be subjected to direct impact with the ground if this orientation was maintained until impact. Even with a large parachute to

slow the decent there is a strong probability that at least the propeller if not other components would be severely damaged. One possibility is to use the parachute to reorientate the vehicle prior to landing. This could be done by having the parachute eject from the side of the center post just above the propeller and electric motor. Once the parachute is deployed it would flip the vehicle so that the cross members are now at the bottom. An added possibility with this approach is to mount all of the equipment including the propeller and electric motor on a platform which could slide down the central post. Once the vehicle is inverted the propeller and all the other components would slide to the bottom of the post and rest up against the main cross members. A mechanism would be used to lock the components in place. This has the added benefit of protecting all of the equipment and propeller in the event the vehicle tumbles upon landing. In order to accomplish this rotation of the vehicle and movement of the experimental package the propeller must be capable of being stopped and held in a known fixed position. This position will have to be predetermined so that it does not interfere with the deployment of the parachute or the movement of the experimental package to the base of the vehicle once the vehicle is reoriented.

The second conceptual design, shown in figure 37, was given the name "spider". This conceptual design was done in order to address some of the issues of propeller and equipment protection associated with the "dart" design. The "spider" platform consists of a central support approximately 3 m (10ft), similar to the "dart" configuration. On the end of this central support the propeller and motor will be attached. Above them located on platforms attached to the main support are racks which contain the batteries, control equipment and data collection devices. The balloon, which is used to carry the platform to its drop altitude, is attached at the top of the central support. Also connected near the top of the support are four hinged arms. Each arm is made up of two segments. The upper segment is hinged at the top of the central support and extends at an angle away form it. It is approximately 3.5 m (11.5 ft) long. The second segment, approximately 3 m (10 ft) long, is rigidly attached to the first segment and is oriented parallel to the central post. When the vehicle is released from the balloon at altitude the four hinged arms raise up above the propeller location, so that they do not interfere with its operational performance. The arms are designed so that the drag force on them is greater then that on the main body of the vehicle. It is this drag force which pushes the arms up into their raised position. Once the testing is complete a parachute is ejected from the top of the central post. This parachute slows the vehicle down for landing. Due to the large drag force generated by the parachute the central support will rise up. The arms will pivot downward and will now be surrounding the central support and propeller . The arms will then be locked into this position. Upon landing the arms will impact the ground and effectively form a cage around the propeller and testing equipment protecting them form impact.

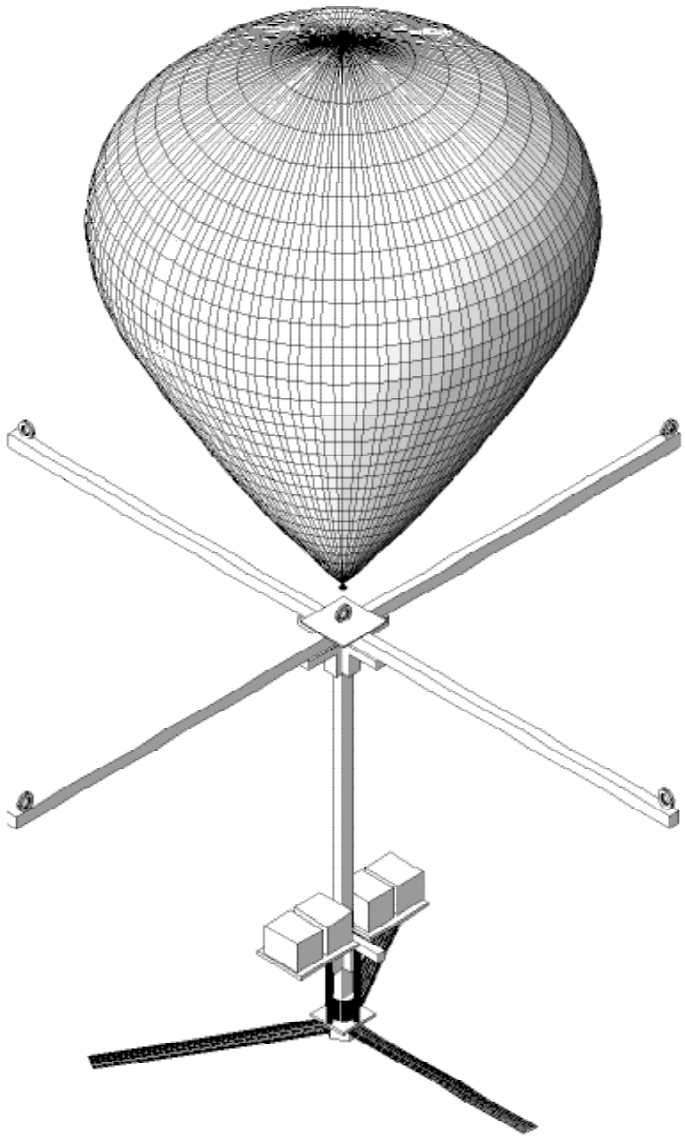

Figure 36 Platform Conceptual Design : Dart Shape

The main drawback to this proposed atmospheric drop test is that the time period for data collection is very short. Since it would not be possible to change propeller pitch angles or rpm during the test only a single propeller operating point will be able to be analyzed. This point most likely would be the design cruise point for the propeller. The information gained from this type of testing would be akin to a yes or no answer as to weather the propeller is operating as expected. The cost of designing and producing this platform was estimated to be on the order of $500,000. This estimate was obtained through discussions which were

held with personnel from the aeronautics group, controls group and engineering directorate form the NASA Lewis Research Center. The balloon and its support facilities cost approximately $30,000 per flight. Due to these costs and the number of drop tests required the ability to generate a performance map for a propeller using this type of testing would not be feasible.

If, after testing, it turns out that there is a problem with the propeller performance not enough data will have been gathered to accurately diagnose the problem. In order to gather more insight into any performance problems a video camera will be mounted to observe the propeller during the drop test. This camera could give some indication to the structural state of the propeller during operation and could indicate weather any performance problems are caused in part by the propellers structural integrity.

This atmospheric drop testing concept has been brought to the conceptual design stage. There is no indication to date that the approach presented above cannot be performed. However, due to the cost involved with this testing approach and the limited amount of data gathered during each test it may prove cost and time effective to seek out an alternate approach to the propeller testing. Other options such as the wind tunnel testing, described in sections 5.2.1 and 5.3.1, and computer modeling, described in section 4.0, should be thoroughly investigated in order to determine if an easier more cost effective approach is available to provide the desired propeller performance data. If, after considering these other methods, there is still sufficient interest to pursue this atmospheric drop testing approach then the next step would be to put together a design team and begin a detailed design of the platform and associated control and data collection systems, based on one of the conceptual designs .

6 Conclusion and Recommendations

The design and prediction of a propeller's performance at high altitudes is much different than that of a conventional propeller operating at lower altitudes. The main reason for this difference is the aerodynamic regime in which the propeller must operate. The operational Reynolds number of a high altitude propeller is much less than that of a conventional propeller. This low Reynolds number operation is due mainly to the low atmospheric density at the higher altitudes. Also due to the size of a high altitude propeller, the tip speed of the propeller approaches the speed of sound during operation. This combination of low Reynolds number and high subsonic Mach number make the design and operation of a high altitude propeller very unique. Based on the various design and analysis approaches given throughout this overview some recommendations can be made regarding the ability to evaluate a propeller for the ERAST mission. The complete design and construction of a propeller is a fairly substantial task. The two cost estimates which were obtained were both around $1 million dollars and required a time frame of between 1 to 2 years. If the resources are not available to perform this type of design then setting up the capability to analyze an existing propeller design is probably the next best approach. A possible

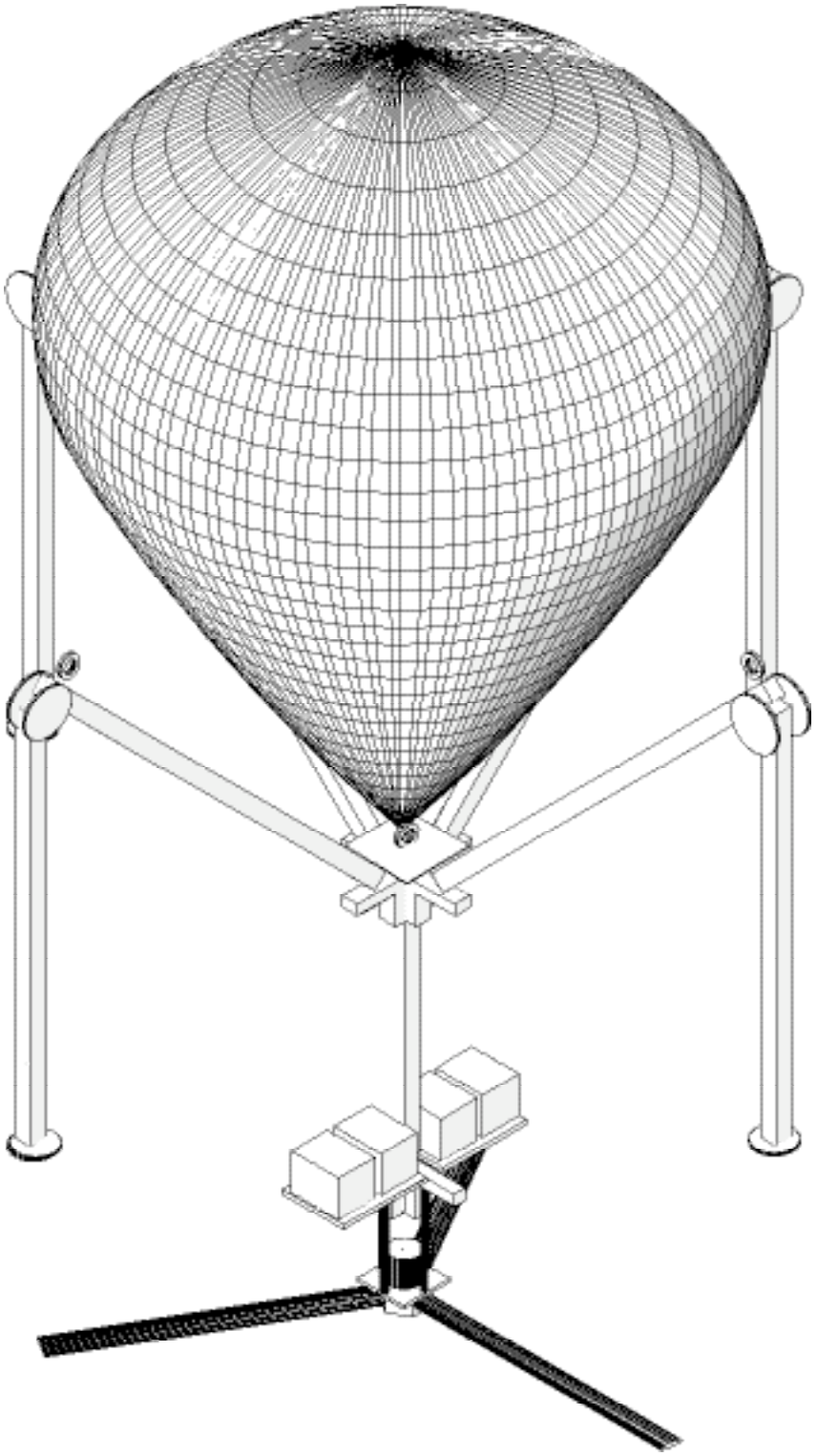

Figure 37 Platform Conceptual Design : Spider Shape

candidate is the CONDOR propeller. This possibility was examined in section 3.3 and further analysis should be done on this propeller to get a more accurate prediction of its performance at altitudes upwards of 24 km (80 kft). This further analysis would require knowledge of the structural makeup of the propeller which to date has not been obtained.

There are two main approaches to analyzing a given propeller design, experimentation and computer modeling. The problem with the computer models is that there is no experimental data available to validate the various computer codes for operation within the low Reynolds number, high subsonic Mach number regime. Therefore some experimentation is needed to either use the computer analysis capabilities with confidence or produce data directly. There are however issues with the use of experimental facilities. The facilities must be pressurized in order to meet the Reynolds number requirement while maintaining a reasonable test sample size. The test section must be large enough to accommodate the test sample. And the turbulence level of the flow field must be very low. Due to these constraints the ability to find a tunnel capable of testing a complete propeller is probably not likely. The most cost effective and beneficial approach to the experimental testing is to perform a 2D airfoil test. This testing can produce data which can be used to validate the 2D airfoil analysis codes. Once validated these codes can be used to generate airfoil data which can be used in conjunction with a strip or vortex theory code to provide propeller performance estimates. This will establish the capability to quickly and fairly accurately analyze a propellers performance. Although not as accurate as a full 3D test the 2D airfoil data is a reasonable compromise due to the difficulty and cost associated with a full propeller analysis. If full propeller testing is warranted and a capable wind tunnel cannot be found then the proposed drop test experiment can be performed. This test should be performed as a last resort due to the cost involved with designing and constructing the platform , approximately $500,000 , the balloon costs per drop, approximately $30,000, and the limited data collected per test.

In summary based on the current status and requirements of the ERAST program it is recommended that a 2D airfoil experimentation be undertaken to generate data on various airfoils at low Reynolds numbers and high subsonic Mach numbers. This data will be useful in establishing an analysis capability as well as contributing to the field of aeronautics by providing data in a regime previously uninvestigated.

7 Reference

1. NASA Lewis Research Center Internet Web Site on the ERAST Program, http://powerweb.lerc.NASA.gov/psi/DOC/erast.html.

2. Airborn Research Australia internet web site, http://www.es.flinders.edu.au/ARA/overview/23.html

3. Studebaker, K. and Matuska, D., "Variable Diameter Tiltrotor Wind Tunnel Test Results," Presented at the American Helicopter Society 49th Annual Forum, May 1993.

4. Fradenburgh, E.A. and Matuska, D.G., "Advanced Tiltrotor State-of-the-Art with Variable Diameter Rotors," Presented at the American Helicopter Society 48th Annual Forum, June 1992.

5. Hutchison,R.A. and Turner, L. Internal Boeing Report, "Propulsion System Final MDS Report," L-1613-GWNL90-024, March 30, 1990.

6. McCormic,B.W., Aerodynamics,Aeronautics and Flight Mechanics, John Wiley and Sons, New York, 1979.

7. Henry V. Borst and Associates, "Aerodynamic Design and Analysis of Propellers for Mini-Remotely Piloted Air Vehicles," Final Report USAAMRDL-TR-77-45A, January 1978.

8. Eppler,R.,Somers,D.M.,"A Computer Program for the Design and Analysis of Low-Speed Airfoils," NASA TM-80210, August 1980.

10. Koch, L.D., "Desing and Performance Calculations of a Propeller for Very High Altitude Flight," Master of Science in Engineering Thesis, Case Western Reserve University, January 1998.

12. Drela,M. and Giles,M.B.,"Viscous-Inviscid Analysis of Transonic and Low Reynolds Number Airfoils," AIAA Journal, 25(10), pp.1347-1355, October 1987.

13. Drela, M. "Integral Boundary Layer Formulation for Blunt Trailing Edges," AIAA-89-2200, August 1989.

14. Drela, M. "A User's Guide to MSES 2.95," MIT Computational Aerospace Sciences Laboratory, September 1996.

15. Drela, M. "A User's Guide to AIRSET V2.3," MIT Computational Aerospace Sciences Laboratory, June 1996.

11. Drela, M. "XFOIL 6.8 User Primer," MIT Computational Aerospace Sciences Laboratory, September 1996.

9. Hall,E.J., Topp, D.A. and Delaney, R.A., Allison Engine Company, "ADPAC User's Manual," NASA CR-195472, April 1996.

16. Warsi, S.A., "User's Guide to PMESH - A Grid Generation Program for

Single-Rotation and Counterrotation Advanced Turboprops," NASA CR-185156, December 1989.

17. Miller,D.P.,"TIGGERC - Turbomachinery Interactive Grid Generator for 2-D Grid Applications and Users Guide," NASA TM-106586, May 1994.

18. Toot,P.L., "Summary of Experimental Testing of a Transonic Low Reynolds Number Airfoil," U.S. Naval Research Laboratory.

19. Selig, M.S., Donovan, J.F., Fraser, D.B., "Airfoils at Low Speeds," Soartech 8, H.A. Stokely, publisher, 1989.

20. Britcher, C.P. "Possibilities for Aerodynamic and Heat Transfer Testing of ERAST Components in the NASA Langley Transonic Dynamics Tunnel," Department of Aerospace Engineering, Old Dominion University.

21. Cole,S.R. and Rivera, J.A. Jr,"The New Heavy Gas Testing Capability in the NASA Langley Transonic Dynamics Tunnel," Forum Paper No.4, Royal Aeronautical Society, Wind Tunnels and Wing Tunnel Test Techniques Forum, April 1997.

22. Langley Working Paper, " The Langley Transonic Dynamicw Tunnel, NASA Langley Research Center Sept, 1969.

23. Gieer, J, "APEX, Aerodynamic Research Objectives and Requirements Document," NASA Dryden Flight Research Center.

24. "NSBF Information Package FY 98," National Scientific Balloon Facility, Palestine, Texas, 1998.

Appendix A: Condor MDS Report Data

APPENDIX OMITTED DUE TO EXPORT CONTROL

Appendix B: Propeller Performance Analysis Source Code.

```
/* written by Anthony Colozza
NYMA Inc. NASA Lewis Research Center Group
Phone (216) 433-5293
21000 Brookpark Road
Mail Stop 301-3
Email a.colozza@lerc.NASA.gov
Cleveland Ohio 44135

Last Modified 11/13/97 */

/* This program determines the efficiency and thrust for a propeller using
either the momentum - blade element theory or vortex theory with or without
small angle simplifying assumption. */
```

```
/*      Note to change the type of propeller used or its geometry the program must be edited
        this consists of changing whichever of the following lines are necessary
        propeller airfoil lift curve slope (a) and any post stall curve data (line 114 and lines 267 -
        281),
        airfoil maximum lift coefficient (line 119)
        propeller hub diameter (rh) (line 115),
        Propeller blade twist function (beta) which includes a curve fit for thickness/c (line 166),
        Propeller chord length function (c) (line 174),
        Propeller airfoil cd vs cl curve fit (line 286)

        Note remember to adjust post clmax calculation to match post stall cl alpha curve    */

/*      Note that the Propeller Diameter and Number of blades are inputs and therefore
        do not require any editing */


//  added to the code was a curve fit to account for the possibility of low Reynolds number flow.

#include  <stdio.h>
#include  <stdlib.h>
#include  <math.h>


main  ()

{
        float  a,af,alpha,alphai,alphaisa,beta,c,cl,clmax,cd,ct,cp,d,dalpha,dx,dy,deltacp,
        deltact,dens,eff,f,fie,fiet,gasc,gamma,h,h1,i,j,jint,jfin,lambda,method,nblds,omega,
        pi,pin,puse,pitch,pitchd,r,re,rpm,rh,sigma,sig,t,term1,term2,thrust,tmach,test1,test2,
        v,vr,vt,wa,wt,wasa,wtsa,x,xx,y,yy;

        char name[80];

        FILE *fp;

        printf("Enter the output data file name\n");
        scanf("%s",name);

        fp=fopen(name,"w");
        printf("Enter altitude in km\n");
        scanf("%f",&h1);

        printf("Enter the initial advance ratio\n");
        scanf("%f",&jint);

        printf("Enter the final advance ratio\n");
        scanf("%f",&jfin);

        printf("Enter propeller diameter in m\n");
        scanf("%f",&d);
```

```
        printf("Enter the number of propeller blades\n");
        scanf("%f",&nblds);

        printf("Select the analysis method you wish to use.\n");
        printf("They are listed in order of complexity lowest (quickest)\n");
        printf("to highest (slowest)\n");
        printf("Enter 1 for Momentum Blade Element Theory Analysis\n");
        printf("Enter 2 for Vortex Theory Analysis with Small Angle Assumption\n");
        printf("Enter 3 for Vortex Theory Analysis\n");
        scanf("%f",&method);


        re=6378000;         /* mean radius of earth m */
        pi=3.14159;


/* Atmospheric Density and Temperature Calculations */

                gasc=287;
                gamma=1.4;
                h1=h1*1000;
                h=re*h1/(re+h1);

                if(h1 <= 11000) {
                        t=288.15-0.0065*h;
                        sig=pow(288.15/t,-4.255876);
                }

                if(h1>11000 && h1<= 20000) {
                        t=216.65;
                        sig=0.297277*exp((11000-h)/6341.62);
                }

                if(h1>20000 && h1 <= 32000) {
                        t=216.65 + (h-20000)/1000;
                        sig=0.07186531*pow(216.69/t,35.16319);
                }

                if(h1>32000 && h1 <= 47000) {
                        t=228.65+2.8*(h-32000)/1000;
                        sig=0.01079592*pow(228.65/t,13.20114);
                }
                dens=sig*1.225;


/*      propeller and airfoil constants */

        a=6.207;                /* propeller airfoil lift curve slope in cl/radian */
        rh=.30;                 /* propeller hub radius in meters */

        tmach =.70;             /*tip Mach number */
        r=d/2;                  /*propeller  radius*/
```

```
        clmax=1.2;              /* maximum lift coefficient */

        dx=0.01;

        fprintf(fp,"altitude (km) %4.1f\n",h1/1000);
        fprintf(fp,"propeller diameter (m) %4.2f\n",d);
        fprintf(fp,"number of blades %3.0f\n",nblds);
        fprintf(fp,"propeller RPM %7.2f\n",rpm);

        pitchd=10;
        while (pitchd <=50) {

        printf("pitch angle deg %5.2f\n",pitchd);
        j=jint;

        pitch=pitchd*pi/180;
        fprintf(fp,"pitch angle degrees %5.2f\n",pitchd);
        fprintf(fp,"\n");

        fprintf(fp,"advance ratio efficiency     ct     cp    T(lbs)    P(hp)");
        fprintf(fp,"      v(m/s)\n");

        while (j <=jfin)        {

        rpm= tmach*60*sqrt(gamma*gasc*t)/(pow(pow(pi,2)+pow(j,2),.5)*d);
        omega=rpm*2*pi/60;          /*angular velocity in radians per second */

        vt=omega*r;

        ct=0.0;
        cp=0.0;
        v=j*rpm*d/60;
        lambda=v/(omega*r);
        x=rh/r;

        while (x<=1) {

        vr=vt*sqrt(pow(x,2)+pow(lambda,2));
        fie=atan(lambda/x);

/*equation for blade twist as a function of x  (note the curve fit is for a .75 chord angle of 15°
therefore 15° must be subtracted form the curve fit to account for just the angle change due to
twist)*/

                beta= pitch + (0.64112 + 0.71602*x - 5.1362*pow(x,2) + 6.7878*pow(x,3) -
                2.8149*pow(x,4)) + (3.4039 - 23.607*x + 67.301*pow(x,2) - 95.672*pow(x,3) +
        67.982*pow(x,4) - 18.855*pow(x,5))*pi/180 - 15*pi/180;


/*chord length as a function of normalized radial distance (r/R) */
        c=(0.084241 - 0.85789*x + 4.7176*pow(x,2) - 9.6225*pow(x,3) + 8.5004*pow(x,4) -
        2.7959*pow(x,5))*d;
```

```
af = (100000/16)*(0.084241/3 - 0.85789/4 + 4.7176/5 - 9.6225/6 + 8.5004/7 - 2.7959/8);

sigma=nblds*c/(pi*r);


/* calculation for propeller efficiency and thrust using Momentum - Blade
        element theory */


if (method == 1) {

alphai=.5*(-1*(lambda/x+sigma*a*vr/(8*pow(x,2)*vt)) +
sqrt(pow(lambda/x+sigma*a*vr/
(8*pow(x,2)*vt),2) + sigma*a*vr*(beta-fie)/(2*pow(x,2)*vt)));

wt=vr*alphai*sin(fie+alphai);
wa=vr*alphai*cos(fie+alphai);
}

if (method>1) {

fiet=atan(lambda);
f=2*acos(exp((x-1)*nblds/(2*sin(fiet))));
xx=lambda/x+a*sigma/(8*x*f*cos(fiet));
yy=sigma*a*(beta-fie)/(8*x*f*cos(fie));
alphai=.5*(sqrt(pow(xx,2)+4*yy)-xx);
wt=alphai*vr*sin(fie+alphai);
wa=vr*alphai*cos(fie+alphai);
alphaisa=alphai;
wtsa=wt;
wasa=wa;
}

if (method == 3) {
wt=wt-.1*wt;
i=0;
while (i<=100){

        test1 = pow(v,2)+4*wt*(omega*r*x-wt);
        test2 = pow(lambda,2)+4*wt*(x-wt/vt)/vt;

        if ( test1 < 0.0 || test2 < 0.0) {
        wt = wtsa;
        wa = wasa;
        break;
        }

        term1=sqrt(pow(v,2)+4*wt*(omega*r*x-wt))-v;
        term2=lambda+sqrt(pow(lambda,2)+4*wt*(x-wt/vt)/vt);

        y=sigma*a*(beta-atan(wt*2/term1))*sqrt(.25*pow(term2,2)+pow(x-wt/vt,2))-
```

```
                8*x*f*wt/vt;

                dy=sigma*a*((.5*pow(pow(v,2)+4*wt*(omega*r*x-wt),-.5)*2*wt*(4*omega*r*x-
8*wt)-
                2*term1)*sqrt(.25*pow(term2,2)+pow(x-wt/vt,2))/(4*pow(wt,2)+pow(term1,2))+
                (beta-atan(2*wt/term1))*.5*pow(.25*pow(term2,2)+pow(x-wt/vt,2),-.5)*
                (.25*term2*pow(pow(lambda,2)+4*wt*(x-wt/vt)/vt,-.5)*(4*x/vt-8*wt/pow(vt,2))+
                2*(wt/pow(vt,2)-x/vt)))-8*x*f/vt;

                if(fabs(y/dy)<=.01){
                break;
                }

                wt=wt-y/dy;

                if (i>=100) {
                        printf("no solution was found for wt, program has terninated  ");
                        printf("x value at termination was %5.3f\n",x);

                        abort();

                        }

                i=i+1;

                }

                wa=.5*(sqrt(pow(v,2)+4*wt*(omega*r*x-wt))-v);
                alphai=atan(wt/wa)-fie;
                if (alphai < 0){
                        wt=wtsa;
                        wa=wasa;
                        alphai=alphaisa;
                }

        }
        dalpha=2*wt*(v+wa)/(omega*r*x*(omega*r*x-2*wt)+pow(v+wa,2));

        alpha = beta-fie-alphai-dalpha;
        cl=a*alpha;

/* post stall airfoil characteristics using a curve fit for approximate cl values */

        if (alpha > 10*pi/180 && alpha <= 15*pi/180) {
                cl=clmax;
        }

        if (alpha > 15*pi/180 && alpha <= 20*pi/180) {
        cl = 0.24/(pi/180) *alpha - 4.8;
        }

        if (alpha > 20*pi/180) {
```

```
        cl = 0.0;
        }

        if (cl < 0.0) {
        cl = 0.0;
        }

/*the equation for cd is a curve fit of the cl vs cd for the airfoil
          being used */

        cd=0.013105 - 0.011179*cl + 0.0060273*pow(cl,2) + 0.004034*pow(cl,3) + 0.0046528*pow(cl,4);



        deltact=(pi/8)*(pow(j,2)+pow(pi*x,2))*sigma*(cl*cos(fie+alphai+dalpha)-
        cd*sin(fie+alphai+dalpha))*dx;

        if (deltact < 0) {
         deltact=0.0;
         }

        deltacp=(pi/8)*(pi*x)*(pow(j,2)+pow(pi*x,2))*sigma*(cl*sin(fie+alphai+dalpha)+
        cd*cos(fie+alphai+dalpha))*dx;

        if (deltacp < 0) {
        deltacp=0.0;
        }

        ct=ct+deltact;
        cp=cp+deltacp;

        x=x+dx;

        }

        thrust=ct*dens*pow(rpm/60,2)*pow(d,4);
        pin=cp*dens*pow(rpm/60,3)*pow(d,5);
        puse=thrust*v;
        eff=puse/pin;

        printf("Thrust Produced N,lbf          %8.2f   %8.2f\n",thrust,thrust/4.448);
        printf("Shaft Power Required kW, hp%8.2f   %8.2f\n",pin/1000,pin/(.7457*1000));
        printf("Propeller Efficiency   %5.4f\n",eff);
        printf("Thrust Coefficient     %5.4f\n",ct);
        printf("Pressure Coefficient   %5.4f\n",cp);
        printf("rpm    %6.2f\n",rpm);
        printf("velocity m/s  %6.2f\n",v);
        printf("advance ratio  %5.2f\n",j);

        fprintf(fp,"    %4.2f      %5.4f     %5.4f    %5.4f  %8.2f %8.2f   %6.2f\n"
        ,j,eff,ct,cp,thrust/4.448,pin/(.7457*1000),v);
```

```
/* set increment for advance ratio j */

        j=j+.05;


        }

/* set increment for propeller pitch */

        pitchd=pitchd+2;

        }

        }
```

Appendix C: Sample Input and Output for Eppler Airfoil Analysis Code

First Input file for Eppler Airfoil analysis code providing angle of attack and Reynolds number range to be analyzed.

```
FXPR14
ALFA113  5  200  400  600  800 1000
RE  120   0000  10000000   5000000   2500000   2000000   150
ENDE
```

Second input file for Eppler airfoil analysis code providing airfoil geometry.

```
FX63-137B
   49
   1.00000  0.00000
   0.99813  0.00273
   0.99524  0.00403
   0.99004  0.00599
   0.97848  0.00989
   0.94758  0.01889
   0.90432  0.03103
   0.83405  0.05027
   0.76242  0.06743
   0.68583  0.08408
   0.60394  0.09972
   0.53476  0.10971
   0.45272  0.11760
   0.37524  0.12111
   0.28888  0.11925
   0.21585  0.11169
   0.14628  0.09767
   0.10000  0.08367
   0.06262  0.06835
```

```
0.03783  0.05437
0.01623  0.03577
0.00468  0.01975
0.00118  0.01032
0.00000  0.00000
0.00160 -0.00614
0.00333 -0.00861
0.00675 -0.01148
0.01140 -0.01432
0.01857 -0.01727
0.03606 -0.02178
0.06990 -0.02781
0.11115 -0.03047
0.15725 -0.02833
0.20042 -0.02754
0.28516 -0.02414
0.36884 -0.01684
0.45637 -0.00716
0.53717  0.00236
0.63054  0.01208
0.70945  0.01889
0.79234  0.02205
0.86207  0.02006
0.91819  0.01416
0.95596  0.00762
0.97732  0.00321
0.99003  0.00034
0.99535 -0.00083
0.99817 -0.00141
1.00000  0.00000
```

Appendix C: Condor Propeller Geometry Data

APPENDIX C OMITTED DUE TO EXPORT CONTROL

Appendix D Input Geometry Conversion Program for CH Grid

```
/* written by Anthony Colozza
              NYMA Inc. NASA Lewis Research Center Group
              21000 Brookpark Road
              Cleveland Ohio 44135          * /


 / *     This program sets up the input file for the grid generator CH Grid */

#include <stdio.h>
#include <stdlib.h>
#include <math.h>
```

```
main ()

{

float afx[780],afs[780],angup,angdn,beta,cup[13][31],cdn[13][31],cdntot[13][61],cuptot[13][61],
        chord,dia,deltax,r,ra[64],rs[13],rup[13][31],rdn[13][31],thaup[13][31],thadn[13][31],
        x[13][31],xa[64],xlimit,xh,xup[13][31],xdn[13][31],xtot[13][61],temp;

int a,aa,b,c,d,e,f,g,count,count2,i,j,jj,k,kk,p,ptc,pt1,pt1old,q,qq,nap,nh,npx,nrs,nxp,ref,rev,
        totalpts,z,zz,temp2;

char name[80], afinput[80];

        FILE *fp, *fpa;

        printf("Enter the output data file name\n");
        scanf("%s",name);

        printf("Enter the airfoil data file name\n");
        scanf("%s",afinput);

        printf("Enter the propeller diameter in m\n");
        scanf("%f",&dia);

        printf("Enter the number of hub data points\n");
        scanf("%d",&nh);

        printf("Enter the total number of data points for the airfoil (top and bottom)\n");
        scanf("%d",&nap);

        printf("Enter the number of x axis data points\n");
        scanf("%d",&nxp);

        printf("Enter the number of radial stations for the airforl\n");
        scanf("%d",&nrs);
        fp=fopen(name,"w");
        fpa=fopen(afinput,"r");
xh=-1.5;
xlimit=2.0;
i=1;
/*initial all arrays to zero */
zz=1;
while (zz <= 15){
        z=1;
        while (z <= 50){
                cup[zz][z]=1.00000;
                cdn[zz][z]=1.00000;
                x[zz][z]=1.00000;
                xup[zz][z]=1.00000;
                xdn[zz][z]=1.00000;
        z=z+1;
```

```
        }
zz=zz+1;
}
z=1;
while(z <= 400){
        afx[z] = 1.00000;
        afs[z] = 1.00000;
        z=z+1;
}
z=1;
while(z <= 100) {
        xa[z] = 1.0000;
        ra[z] = 1.0000;
        z=z+1;
}
*/
deltax=(xlimit-xh)/nh;
/* generate hub coordinate values */
while(xh<=xlimit){
/*equation for the hub*/
r= .03*atan(2.5*(xh+.5))+.035*atan(2);
ra[i]=r;
xa[i]=xh;
xh=xh+deltax;
i=i+
}
k=1;
kk=1;
while(k <= nh){
        if(kk==9){
                fprintf(fp,"\n");
                kk=1;
        }
        fprintf(fp,"  %8.5f",xa[k]);
        kk=kk+1;
        k=k+1;
}
j=1;
jj=1;
fprintf(fp,"\n");
while(j <= nh){
        if(jj==9){
                fprintf(fp,"\n");
                jj=1;
        }
        fprintf(fp,"  %8.5f",ra[j]);
        jj=jj+1;
        j=j+1;
}
totalpts = nrs*nap;
p=1;
b=1;
```

```
fprintf(fp,"\n");
/* read in and output airfoil data */
while(b <= nrs){
        fscanf(fpa,"%f",  &rs[b]);
        printf("%d %f \n",b,rs[b]);
        b=b+1;
}
while(p <= totalpts){
        fscanf(fpa,"%f  %f",&afx[p],  &afs[p]);
        /*printf("%d %f %f \n",p,afx[p],afs[p]);*/
        p=p+1;
        }
ref=0;
q=0;
qq=1;
while(qq <= nrs){
q=1;
ref=ref+q-1;
count2=0;
        while(q <= nap){
                if(q <= nxp){
                        x[qq][q]=afx[q+ref];
                        cup[qq][q]=afs[q+ref];
                }
                if(q > nxp)
                        cdn[qq][nxp-count2]=((afs[q+ref+1]-afs[q+ref])/(afx[q+ref+1]-afx[q+ref]))*
                        (x[qq][nxp-count2]-afx[q+ref+1])+afs[q+ref+1];
                        if(nxp-count2 == 1){
                                cdn[qq][nxp-count2]=((afs[q+ref]-afs[q+ref-1])/(afx[q+ref]-
afx[q+ref-1]))*
                        (x[qq][nxp-count2]-afx[q+ref])+afs[q+ref];
                        }
                        /*printf(" %d  %d %d %d %f %f %f %f \n",
                        qq,q,count2,ref,afs[q+ref+1],afs[q+ref],afx[q+ref+1],afx[q+ref]);*/
                        count2=count2+1;
                }
                q=q+1;
        }
        qq=qq+1;
}
/* for airfoils normalized from 0 to 1 they must be shifted to -.5 to .5
 curve fit adjustment to the chord length of each blade section
 rotation of the airfoil section */
aa=1;
while(aa <= nrs){
        chord = 0.06133+0.25404*rs[aa]+1.6464*pow(rs[aa],2)-5.6698*pow(rs[aa],3)
                 +6.1367*pow(rs[aa],4)-2.39*pow(rs[aa],5);
        beta = 1.2714 - 2.5541*rs[aa] + 2.0236*pow(rs[aa],2) - 0.66036*pow(rs[aa],3);
        a=1;
        printf("chord,  %f\n",chord);
        printf("beta,  %f\n",beta);
        while(a <= nxp){
```

```
                x[aa][a]=((x[aa][a]-.5)*chord/dia);
                cup[aa][a]=(cup[aa][a]*chord/dia);
                cdn[aa][a]=cdn[aa][a]*chord/dia;
                rup[aa][a]=pow(pow(cup[aa][a],2)+pow(x[aa][a],2),.5);
                angup=atan(cup[aa][a]/x[aa][a]);
                if(angup < 0){
                        angup=3.141592654+angup;
                }
                thaup[aa][a]=angup+beta;
                rdn[aa][a]=pow(pow(cdn[aa][a],2)+pow(x[aa][a],2),.5);
                angdn=atan(cdn[aa][a]/x[aa][a]);
                /*printf(" %d  %d  %f  %f  \n",aa,a,x[aa][a],cdn[aa][a]);*/
                if(angdn < 0){
                angdn= 3.141592654+angdn;
                }
                thadn[aa][a]=angdn+beta;
                xup[aa][a]=rup[aa][a]*cos(thaup[aa][a]);
                cup[aa][a]=rup[aa][a]*sin(thaup[aa][a]);
                xdn[aa][a]=(rdn[aa][a]*cos(thadn[aa][a]))*-1;
                cdn[aa][a]=(rdn[aa][a]*sin(thadn[aa][a]))*-1;
                /*printf(" %d  %d  %f  %f  %f  %f %f %f  \n",
                aa,a,xup[aa][a],xdn[aa][a],cup[aa][a],cdn[aa][a],rdn[aa][a],thadn[aa][a]);*/
                /*xup[aa][a]pow(pow(cup[aa][a],2)+pow(x[aa][a],2),.5)*
                cos(atan(cup[aa][a]/x[aa][a])+beta);
                cup[aa][a]=pow(pow(cup[aa][a],2)+pow(x[aa][a],2),.5)*
                sin(atan(cup[aa][a]/x[aa][a])+beta);
                xdn[aa][a]=pow(pow(cdn[aa][a],2)+pow(x[aa][a],2),.5)*
                cos(atan(cdn[aa][a]/x[aa][a])+beta);
                cdn[aa][a]=pow(pow(cdn[aa][a],2)+pow(x[aa][a],2),.5)*
                sin(atan(cdn[aa][a]/x[aa][a])+beta);
                temp = cos(atan(cdn[aa][a]/x[aa][a])+beta);*/
                a=a+1;
        }
        c=1;
        e=1;
        /*combine upper and lower coordinate points into a single set and organize them with
increasing x values */
        while(c <= nxp){
                d=
                while(d <= nxp){
                if (xdn[aa][d] > xup[aa][c] && xdn[aa][d] != 10) {
                        xtot[aa][e]=xdn[aa][d];
                        cdntot[aa][e]=cdn[aa][d];
                        cuptot[aa][e]=10;
                        e=e+1;
                        xdn[aa][d] = 10;
                }
                d=d+1;
                }
                xtot[aa][e]=xup[aa][c];
                cuptot[aa][e]=cup[aa][c];
                cdntot[aa][e]=10;
```

```
        /*printf(" %d   %d   %f   %f  %f   \n",aa,e,xtot[aa][e],cuptot[aa][e],cdntot[aa][e]);*/
        e=e+1;
        c=c+1;
}
rev=0;
f=1;
count = 1;
/* do a linear interpolation for mission upper  points for each x value */
while(f <= nxp*2){
        if(cuptot[aa][f] != 10 && count ==2){
                ptc = pt1+1;
                if(rev==1){
                        while(rev<pt1){
                                cuptot[aa][rev]=(cuptot[aa][pt1]-cuptot[aa][f])*(xtot[aa][rev]-
                                xtot[aa][pt1])/
                                (xtot[aa][pt1]-xtot[aa][f])+cuptot[aa][pt1];
                        rev=rev+1;
                        }
                }
                while(ptc < f){
                        cuptot[aa][ptc]=(cuptot[aa][pt1]-cuptot[aa][f])*(xtot[aa][ptc]-
                                        xtot[aa][pt1])/
                                (xtot[aa][pt1]-xtot[aa][f])+cuptot[aa][pt1];
                        ptc=ptc+1;
                }
                pt1old=pt1;
                pt1=f;
        }
        if(cuptot[aa][f] == 10 && f==nxp*2){
                ptc = pt1+1;
                while(ptc <= f){
                        cuptot[aa][ptc]=(cuptot[aa][pt1old]-cuptot[aa][pt1])*(xtot[aa][ptc]-
                                xtot[aa][pt1old])/
                                (xtot[aa][pt1old]-xtot[aa][pt1])+cuptot[aa][pt1old];
                        ptc=ptc+1;
                }
        }
        if(cuptot[aa][f] != 10 && count == 1){
                if(f>1){
                        rev=1;
                }
                pt1=f;
                count=2;
        }
        f=f+1;
}
/* do a linear interpolation for mission lower  points for each x value */
rev=0;
g=1;
count = 1;
while(g <= nxp*2){
                if(cdntot[aa][g] != 10 && count ==2){
```

```
                                        ptc = pt1+1;
                        if(rev==1){
                                while(rev<pt1){
                                cdntot[aa][rev]=(cuptot[aa][pt1]-cuptot[aa][g])*(xtot[aa][rev]-
                                xtot[aa][pt1])/
                                        (xtot[aa][pt1]-xtot[aa][g])+cuptot[aa][pt1];
                                rev=rev+1;
                                }
                        }
                        while(ptc < g){
                                cdntot[aa][ptc]=(cdntot[aa][pt1]-cdntot[aa][g])*(xtot[aa][ptc]-
                                xtot[aa][pt1])/
                                        (xtot[aa][pt1]-xtot[aa][g])+cdntot[aa][pt1];
                                ptc=ptc+1;
                        }
                        pt1old=pt1;
                        pt1=g;
                }
                if(cdntot[aa][g] == 10 && g==nxp*2){
                        ptc = pt1+1;
                        while(ptc <= g){
                                cdntot[aa][ptc]=(cdntot[aa][pt1old]-cdntot[aa][pt1])*(xtot[aa][ptc]-
                                xtot[aa][pt1old])/
                                        (xtot[aa][pt1old]-xtot[aa][pt1])+cdntot[aa][pt1old];
                                ptc=ptc+1;
                        }
                }
                if(cdntot[aa][g] != 10 && count == 1){
                        if(g>1){
                                rev=1;
                        }
                        pt1=g;
                        count=2;
                }
                g=g+1;
        }
        temp2=1;
        while(temp2 <= nxp*2){
                /*printf(" %d   %d   %f   %f  %f
\n",aa,temp2,xtot[aa][temp2],cuptot[aa][temp2],cdntot[aa][temp2]);*/
                temp2 = temp2+1;
        }
        aa=aa+1;
}
jj=1;
while(jj <= nrs){
        j=1;
        k=nxp;
        while(j <= nxp*2) {
                cdn[jj][k]=cdntot[jj][j];
                cup[jj][k]=cuptot[jj][j];
                x[jj][k]=xtot[jj][j];
```

```
                j=j+2;
                k=k-1;
        }
        jj=jj+1;
}
jj=1;
/*fprintf(fp,"\n");*/
while(jj <= nrs){
        j=1;
        count=9;
        while(j <= nxp){
                if(count==9){
                        fprintf(fp,"\n");
                        count=1;
                }
                fprintf(fp,"  %9.6f",x[jj][j]);
                j=j+1;
                count=count+1;
        }
        jj=jj+1;
}
jj=1;
/*fprintf(fp,"\n");*/
while(jj <= nrs){
        j=1;
        count=9
        while(j <= nxp){
                if(count==9){
                        fprintf(fp,"\n");
                        count=1;
                fprintf(fp,"  %9.6f",rs[jj]/2.0 + .03*atan(1.25)+.035*atan(2));
                j=j+1;
                count=count+1;
        }
        jj=jj+1;
}
/*fprintf(fp,"\n");*/
jj=1;
while(jj <= nrs){
        j=1;
        count=9;
        while(j <= nxp){

                if(count==9){
                        fprintf(fp,"\n");
                        count=1;
                }
                fprintf(fp,"  %9.6f",cup[jj][j]);
                j=j+1;
                count=count+1;
        }
        jj=jj+1;
```

```
}
jj=1;
/*fprintf(fp,"\n");*/
while(jj <= nrs){
        j=1;
        count=9;
        while(j <= nxp){
                if(count==9){
                        fprintf(fp,"\n");
                        count=1;
                }
                fprintf(fp,"  %9.6f",cdn[jj][j]);
                j=j+1;
                count=count+1;
        }
        jj=jj+1;
}
fclose(fpa);
fclose(fp);
}
```

Appendix E: Perseus Propeller Input Setup for CH Grid Program

APPENDIX E OMITTED DUE TO EXPORT CONTROL

Appendix F Source Code for Propeller Drop Test Model

```
/*                      Anthony Colozza
                        21000 BrookPark Rd. M.S. 301-5
                        Cleveland, Ohio 44111
                        (216) 433-5293
                        August 3, 1997                          */

/*      This program models a propeller test platform which is dropped from a high altitude
        balloon */

#include <stdio.h>
#include <stdlib.h>
#include <math.h>


main ()

{
```

```
float alt,altg,alton,area,areap,areaplt,cd,dens,diap,dp,dt,dur,duri,dv,dplate,g, pltm,r,sig,
t,tg,tlevel, thrust, vi,v;

char name[80];
 FILE *fp;

 int count, prtstp, prttrg;

 printf("Enter the output data file name\n");
 scanf("%s",name);

fp=fopen(name,"w");

printf("Enter Initial Drop Altitude (km)\n");
scanf("%f",&alt);

printf("Enter Platform Drag Coefficient \n");
scanf("%f",&cd);

printf("Enter Platform Mass (kg)\n");
scanf("%f",&pltm);

printf("Enter Thrust Generated By Propeller (N)\n");
scanf("%f",&tlevel);

printf("Enter Equilivant Flat Plate Area of Platform (m^2)\n");
scanf("%f",&area);

printf("Enter Altitude Motor is Turned on (km)\n");
scanf("%f",&alton);

printf("Enter Duration of Motor Operation (sec)\n");
scanf("%f",&duri);
printf("Enter Parachute Diameter (m)\n");
scanf("%f",&diap);


v=0.0;                  // initial velocity
t=0.0;                  // initial time
dt=0.01;                        // time increment
g=9.81;                 // gravitational constant
r=6378000;     // mean raidu s of earth m

count = 0;
alt = alt*1000;
alton=alton*1000;
dp=0.0;
areap = 3.14159*pow(diap,2)/4;
dur=duri;
prtstp = 100;
areaplt = 0.0;
prttrg = 0;
```

```
fprintf(fp,"Initial Platform Altitude (m)          %8.2f\n",alt);
fprintf(fp,"Platform Drag Coefficient              %6.4f\n",cd);
fprintf(fp,"Platform Mass (kg)                  %7.2f\n",pltm);
fprintf(fp,"Propeller Thrust (N)                %7.2f\n",thrust);
fprintf(fp,"Equilivant Flat Plate Area (m^2)       %7.2f\n",area);

fprintf(fp,"");
fprintf(fp,"");

fprintf(fp,"  Time    Velocity    Indicated     Altitude    Plate Area \n");
fprintf(fp,"   (s)     (m/s)    Velocity (m/s)     (m)       Drag (m^2)\n");
while(alt >0.0) {


/* Atmospheric Density and Temperature Calculations */

        altg=r*alt/(r+alt);

        if(alt <= 11000) {
                tg=288.15-0.0065*altg;
                sig=pow(288.15/tg,-4.255876);
        }

        if(alt>11000 && alt<= 20000) {
                tg=216.65;
                sig=0.297277*exp((11000-altg)/6341.62);
        }

        if(alt>20000 && alt <= 32000) {
                tg=216.65 + (altg-20000)/1000;
                sig=0.07186531*pow(216.69/tg,35.16319);
        }

        if(alt>32000 && alt <= 47000) {
                tg=228.65+2.8*(altg-32000)/1000;
                sig=0.01079592*pow(228.65/tg,13.20114);
        }
        dens=sig*1.225;
        vi = v*pow(sig,0.5);

        if ( alt < alton && dur > 0.0){
                thrust = tlevel;
                areaplt = 2*thrust/(1.18*dens*pow(v,2));

                if (dur == duri)
                        fprintf(fp,"    Motor is Turned On  \n");
                dur = dur - dt;

                if (dur <= 0.0)
                        fprintf(fp,"    Motor is Turned Off  \n");
        }
```

```
        else {
                thrust = 0.0;
                areaplt = 0.0;
        }

        if(alt <= 10000) {
                if (prttrg == 0){
                        fprintf(fp,"    Parachute is Opened  \n");
                        prttrg = 1;
                }
                dp = 1.2*areap*dens*pow(v,2)/2;
                prtstp = 1000;
                }

        /* print results to a file */

        if (count == prtstp ) {

        fprintf(fp,"    %7.2f",t);
                fprintf(fp,"     %7.2f",v);
                fprintf(fp,"        %7.2f",vi);
                fprintf(fp,"         %7.2f",alt);
                fprintf(fp,"     %7.2f\n",areaplt);
                count = 0;

        }

        dplate = .5*areaplt*dens*pow(v,2)*1.18;
        dv = ((pltm*g + thrust - cd*area*dens*pow(v,2)/2 -dp - dplate)/pltm)*dt;
        v = v + dv;
        alt = alt - v*dt;
        count = count +1;
        t=t + dt;

        }

}
```

Appendix G Propeller Atmospheric Drop Test Simulation Code Output

Initial Platform Altitude (m) 30500.00
Platform Drag Coefficient 0.8000
Platform Mass (kg) 250.00
Propeller Thrust (N) 450.00
Equilivant Flat Plate Area (m^2) 3.00

Time (s)	Velocity (m/s)	Indicated Velocity (m/s)	Altitude (m)	Plate Area Drag (m^2)

5.00	48.72	5.82	30377.54	0.00
10.00	95.43	11.72	30015.66	0.00
15.00	138.03	17.74	29429.64	0.00
20.00	174.31	23.80	28645.54	0.00
25.00	202.20	29.71	27700.26	0.00
30.00	220.18	35.13	26639.89	0.00
Motor is Turned On				
35.00	231.36	40.33	25511.73	0.00
40.00	235.50	45.02	24339.69	0.00
45.00	229.42	48.10	23173.91	0.00
50.00	216.85	49.70	22056.38	0.00
55.00	201.36	50.18	21010.36	0.00
60.00	185.55	49.98	20043.42	0.00
Motor is Turned Off				
65.00	168.04	48.38	19155.76	0.00
70.00	151.30	46.37	18359.82	0.00
75.00	139.00	45.09	17635.57	0.00
80.00	129.45	44.26	16965.40	0.00
85.00	121.69	43.70	16338.19	0.00
90.00	115.12	43.31	15746.61	0.00
95.00	109.42	43.01	15185.57	0.00
100.00	104.38	42.79	14651.34	0.00
105.00	99.84	42.60	14141.00	0.00
110.01	95.74	42.45	13652.23	0.00
115.01	91.99	42.31	13183.08	0.00
120.01	88.54	42.20	12731.90	0.00
125.01	85.37	42.10	12297.25	0.00
130.01	82.43	42.01	11877.87	0.00
135.01	79.69	41.93	11472.67	0.00
140.00	77.14	41.86	11080.66	0.00
145.00	74.93	41.67	10700.71	0.00
150.00	73.05	41.58	10330.88	0.00
Parachute is Opened				
199.97	13.24	7.99	9366.30	0.00
249.94	12.73	7.99	8717.40	0.00
299.98	12.27	7.99	8092.65	0.00
350.03	11.85	7.99	7489.96	0.00
400.08	11.46	7.99	6907.54	0.00
450.13	11.10	7.99	6343.77	0.00
500.18	10.77	7.99	5797.20	0.00
550.23	10.46	7.99	5266.71	0.00
600.27	10.17	7.99	4751.05	0.00
650.32	9.90	7.99	4249.31	0.00
700.37	9.65	7.99	3760.58	0.00
750.42	9.41	7.99	3284.05	0.00
800.47	9.19	7.99	2819.00	0.00
850.52	8.98	7.99	2364.80	0.00
900.57	8.78	7.99	1920.80	0.00
950.62	8.59	7.99	1486.49	0.00
1000.67	8.41	7.99	1061.34	0.00
1050.71	8.24	7.99	644.91	0.00
1100.76	8.08	7.99	236.75	0.00